

Eugene Lavretsky

Contents

30.1	Introduction	676
30.2	Aircraft Flight Dynamics Equations of Motion	677
30.3	Simplified Flight Dynamics for Control Design	677
30.3.1	Longitudinal Dynamics	678
30.3.2	Lateral-Directional Dynamics	679
30.3.3	Model Generalizations for Adaptive Control Design	680
30.4	Model Following LQR PI Command Tracking	681
30.4.1	Design Example: Lateral-Directional LQR PI Control with Explicit Model Following	685
30.5	Model Reference Adaptive Control	688
30.5.1	MRAC Design for MIMO Dynamics	690
30.5.2	MRAC Design Modifications for Robustness	694
30.5.3	Observer-Based MRAC Design with Transient Guarantees	697
30.6	Conclusion	709
	References	709

Abstract

This chapter contains a collection of reliable, efficient, robust, and adaptive control methods for aerial vehicles. It begins with a brief overview of flight dynamics models suitable for flight control design. The first control design method represents the well-understood and now-classical linear quadratic regulator (LQR) command tracker, with proportional-integral (PI) feedback connections. Such a system is the backbone of all other methods presented in this chapter. The main intent here is to demonstrate the design of predictable, formally justified, yet numerically efficient flight controllers, with an LQR PI baseline and with a direct model reference adaptive control (MRAC), as an augmentation

E. Lavretsky
Boeing Senior Technical Fellow, The Boeing Company, Huntington Beach, CA, USA
e-mail: eugene.lavretsky@boeing.com

to the baseline. Through extensive simulation, analysis, and actual flight testing, it has been found that (LQR PI + adaptive) – controllers provide robust stability and maintain tracking performance, when operated in the presence of “unknown unknowns” in the vehicle dynamics and in often “unfriendly” operational environment. Finally, a note is in order: All control methods described in this chapter were successfully flight tested and validated on a wide range of aerial vehicles.

30.1 Introduction

Robust control is an online policy capable of regulating systems (such as aerial vehicles) with bounded uncertainties in their dynamics. A robust controller would work satisfactorily for a set of plants, whether linear or nonlinear, while assuming the worst case conditions on uncertainties in the vehicle dynamics. Excluding ad hoc designs, all reliable control methods are model based. One often starts with a mathematical model of the vehicle. Such a model would be valid in a preset domain. The model may or may not be accurate in capturing significant effects in the vehicle dynamics. In order to overcome modeling deficiencies, one should seek a robust solution, designed based on the model, yet capable of controlling the real vehicle, and not just the model. It would also be highly desirable to have a controller whose performance “gracefully degrades” in the presence of uncertainties so that it would not abruptly break down when unprecedented events occur.

Embedding robustness properties into a control solution must be treated as one of the main criteria in any control design. For example, achieving closed-loop stability and tracking performance, while providing adequate stability margins, are the main goals, especially when dealing with linear system approximations of real processes. Methods and techniques to achieve this goal will be provided. Once a robust control solution is found, its robustness properties can be further extended to cover a wider class of uncertainties in the system dynamics. Such a problem could be addressed within the framework of adaptive control. It may allow the designer to cope with unbounded state-dependent nonlinear uncertainties that may exist in the vehicle dynamics.

What is the difference between robust and adaptive controllers? A robust controller is designed to operate under the worst case condition assumption. Such a controller may use excessive actions to accomplish the goal. In contrast, an adaptive controller would try to perform an online estimation of the process uncertainty, and then produce a control input to anticipate, overcome, or minimize the undesirable deviations from the prescribed closed-loop plant behavior. In addition to their adaptive properties, these controllers can be constructed to “learn” or equivalently to remember prior events. In this context, the notion of learning refers to remembering certain patterns, and then acting based on prior knowledge or “memory.” For instance, a tracking error integrator in a feedback loop is a learning controller. It accumulates and integrates regulation errors based on previous and current data.

It will be shown that an adaptive controller represents a nonlinear extension of a linear feedback integrator. In other words, adaptive loops form their output by integrating nonlinear functions of the system tracking errors.

A discussion of whether adaptive controllers outperform robust systems or vice versa is of no merit. One can argue that it is rather a seamless combination of both controllers that works best, in the sense of maintaining closed-loop stability, enforcing robustness to uncertainties, and delivering target performance, all and all while operating in the presence of unanticipated events.

30.2 Aircraft Flight Dynamics Equations of Motion

Six-degrees-of-freedom (6-DoF) rigid aircraft equations of motion can be derived based on Newton's second law of motion. These dynamics are often expressed in the aircraft-fixed body axes coordinate system (Etkin 1982; McRuer et al. 1990; Stevens and Lewis 1992). In general, the 6-DoF equations of motion represent a continuous dynamical multi-input–multi-output system in the standard state-space form,

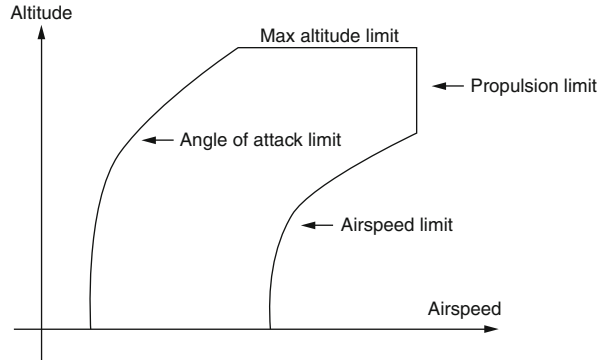
$$\dot{x} = f(x, u), \quad y = h(x, u) \quad (30.1)$$

with the state x , the control input u , and the measured/regulated output y . An attempt to use the fully coupled model (30.1) for control design would most likely result in an impractical control solution of unnecessary complexity and with a highly undesirable sensitivity due to model data. This phenomenon immediately presents a modeling-for-control challenge: How detailed does a control-oriented model need to be, so that the resulting control solution is simple, robust, effective, and works per design specifications, when applied to a real vehicle? The answer to this question of course depends on the application of interest. In the next section, simplified flight dynamics models for control design purposes will be constructed.

30.3 Simplified Flight Dynamics for Control Design

The 6-DoF motion of an aerial vehicle can be decomposed into a mean or a steady-state motion near an operating point (called “trim”) and perturbation dynamics around the trim conditions. Such a decomposition allows one to reduce the overall nonlinear fully coupled 6-DoF aircraft dynamics into a tractable form, suitable for control design and analysis. The notion of “trimming an aircraft” refers to finding a balance, or equilibrium, between aerodynamic, propulsive, and gravitational forces and moments that are constantly acting on the vehicle. In flight, an aircraft is trimmed by setting its primary controls to values that would result in the desired steady-state flight conditions. The trim function would be performed by a pilot or by an automatic flight control system.

Fig. 30.1 Aircraft operational flight envelope, as a function of altitude and airspeed



In mathematical terms, one is looking for a system equilibrium pair $(\vec{x}_{eq}, \vec{u}_{eq})$ in (30.1) such that the translational and angular accelerations are zeroed out:

$$0 = f(x_{eq}, u_{eq}) \quad (30.2)$$

These are steady-state flight conditions. Accelerated flight equilibrium is also possible.

An aircraft would have many distinct equilibrium points throughout the vehicle flight operational envelope (Fig. 30.1).

These trim points depend first hand on altitude and airspeed. Based on available trim flight conditions, the main idea behind constructing control-oriented models and then performing flight control design consists of several distinct steps. They are:

1. Cover the flight envelope with a dense set of trim points.
2. Write simplified linear models around each of the trim point.
3. Use these dynamics to design fixed-point flight controllers per point.
4. Interpolate (i.e., gain schedule based on flight conditions) to combine linear controllers.

The result is a gain-scheduled flight control system that would be valid for the entire operational envelope. In what follows, only Step 2 will be discussed, and linear simplified models (deviation dynamics from equilibrium) for a selected trim point will be defined.

When a conventional aircraft is trimmed wings level, at selected flight conditions, the vehicle dynamics naturally decouples into longitudinal and lateral-directional modes. Each of these modes is presented separately.

30.3.1 Longitudinal Dynamics

The aircraft longitudinal dynamics describe changes in forward, vertical, and pitching motion of the vehicle. These dynamics can be further decomposed into fast and slow components, or modes. The former is called the short-period and the

latter is the phugoid. Typically, there would be a time-scale separation between the two modes. The short-period describes fast coupling between the aircraft angle of attack and the pitch rate. The phugoid represents a much slower (when compared to the short-period) dynamic interchange between the vehicle altitude and airspeed, or, equivalently, between the aircraft potential and kinetic energy levels.

The short-period and the phugoid modes can be revealed after the aircraft model is linearized around a trim point (an equilibrium). For clarity of presentation, it is assumed that the thrust line is aligned with the vehicle x -axis. Then, the aircraft longitudinal equations of motion are

$$\begin{pmatrix} \dot{v}_T \\ \dot{\alpha} \\ \dot{q} \\ \dot{\theta} \end{pmatrix} = \begin{pmatrix} X_V & X_\alpha & 0 & -g \cos \gamma_0 \\ \frac{Z_V}{V_0} & \frac{Z_\alpha}{V_0} & 1 + \frac{Z_q}{V_0} & -\frac{g \sin \gamma_0}{V_0} \\ M_V & M_\alpha & M_q & 0 \\ 0 & 0 & 1 & 0 \end{pmatrix} \begin{pmatrix} v_T \\ \alpha \\ q \\ \theta \end{pmatrix} + \begin{pmatrix} X_{\delta_{th}} \cos \alpha_0 & X_{\delta_e} \\ -X_{\delta_{th}} \sin \alpha_0 & \frac{Z_{\delta_e}}{V_0} \\ M_{\delta_{th}} & M_{\delta_e} \\ 0 & 0 \end{pmatrix} \begin{pmatrix} \delta_{th} \\ \delta_e \end{pmatrix} \quad (30.3)$$

where V_0 is the trimmed airspeed and α_0 is trimmed angle of attack, $\gamma_0 = \theta_0 - \alpha_0$ is the trimmed flight path angle, θ_0 is the trimmed pitch angle, δ_{th} is the throttle position, and δ_e is the elevator position. The model states (v_T , α , q , θ) and the control inputs (δ_{th} , δ_e) are incremental due to their trimmed values. Also in (30.3), the matrix components represent constant (for fixed flight conditions) stability and control derivatives of the aircraft forces and moments, with respect to the longitudinal states and control inputs. When aircraft-specific values of these derivatives are substituted into model (30.3), most often the open-loop system eigenvalues will consist of a fast (short-period) and a slow (phugoid) pair of complex conjugate numbers. Such a decomposition explains the time-scale separation in the longitudinal dynamics of an aircraft.

The short-period mode is defined by the dynamics of α and q . Extracting those from model (30.3) yields

$$\begin{pmatrix} \dot{\alpha} \\ \dot{q} \end{pmatrix} = \begin{pmatrix} \frac{Z_\alpha}{V_0} & 1 + \frac{Z_q}{V_0} \\ M_\alpha & M_q \end{pmatrix} \begin{pmatrix} \alpha \\ q \end{pmatrix} + \begin{pmatrix} \frac{Z_{\delta_e}}{V_0} \\ M_{\delta_e} \end{pmatrix} \delta_e \quad (30.4)$$

These dynamics describe aircraft motion on a short interval of time, due to elevator input. In aerospace applications, the short-period system is utilized quite often to support the development of robust and adaptive control technologies.

30.3.2 Lateral-Directional Dynamics

Assuming constant thrust, airspeed, and angle of attack, lateral-directional dynamics of an aircraft can be derived by linearization of the 6-DoF system (30.2), around a selected trim point. The resulting dynamics are

$$\begin{pmatrix} \dot{\varphi} \\ \dot{\beta} \\ \dot{p}_s \\ \dot{r}_s \end{pmatrix} = \begin{pmatrix} 0 & 0 & \frac{\cos \gamma_0}{\cos \theta_0} & \frac{\sin \gamma_0}{\cos \theta_0} \\ \frac{g \cos \theta_0}{V_0} & \frac{Y_\beta}{V_0} & \frac{Y_p}{V_0} & \frac{Y_r}{V_0} - 1 \\ 0 & L_\beta & L_p & L_r \\ 0 & N_\beta & N_p & N_r \end{pmatrix} \begin{pmatrix} \varphi \\ \beta \\ p_s \\ r_s \end{pmatrix} + \begin{pmatrix} 0 & 0 \\ \frac{Y_{\delta_{ail}}}{V_0} & \frac{Y_{\delta_{rud}}}{V_0} \\ L_{\delta_{ail}} & L_{\delta_{rud}} \\ N_{\delta_{ail}} & N_{\delta_{rud}} \end{pmatrix} \begin{pmatrix} \delta_{ail} \\ \delta_{rud} \end{pmatrix} \quad (30.5)$$

When the airspeed is sufficiently high, the gravity term in (30.5) becomes negligible: $\frac{g \cos \theta_0}{V_0} \approx 0$. In this case, the bank dynamics can be eliminated:

$$\begin{pmatrix} \dot{\beta} \\ \dot{p}_s \\ \dot{r}_s \end{pmatrix} = \begin{pmatrix} \frac{Y_\beta}{V_0} & \frac{Y_p}{V_0} & \frac{Y_r}{V_0} - 1 \\ L_\beta & L_p & L_r \\ N_\beta & N_p & N_r \end{pmatrix} \begin{pmatrix} \beta \\ p_s \\ r_s \end{pmatrix} + \begin{pmatrix} \frac{Y_{\delta_{ail}}}{V_0} & \frac{Y_{\delta_{rud}}}{V_0} \\ L_{\delta_{ail}} & L_{\delta_{rud}} \\ N_{\delta_{ail}} & N_{\delta_{rud}} \end{pmatrix} \begin{pmatrix} \delta_{ail} \\ \delta_{rud} \end{pmatrix} \quad (30.6)$$

The resulting third-order lateral-directional linear model would be suitable for a control design where the goal is to regulate the vehicle roll and yaw rates, as well as the angle of sideslip.

30.3.3 Model Generalizations for Adaptive Control Design

The aircraft short-period dynamics (30.4), as well as the lateral-directional models (30.5) and (30.6), belong to a class of linear time-invariant controllable systems in the form

$$\dot{x} = Ax + Bu \quad (30.7)$$

with the n -dimensional state x , the m -dimensional control u , the p -dimensional output:

$$y = Cx + Du \quad (30.8)$$

and with the matrices (A , B , C , D) of the corresponding dimensions.

In the next section, methods to construct and analyze robust linear LQR-optimal controllers are presented. The focus is on adaptive control techniques, with the goal of maintaining closed-loop stability and robustness in the presence of unexpected events. Specifically, inserting uncertainties into (30.7) and (30.8) results in the dynamical system

$$\dot{x} = Ax + B \Lambda (u + f(x)) \quad (30.9)$$

where the $(m \times m)$ -matrix Λ represents control actuation failures and the m -dimensional state-dependent vector function $f(x)$ denotes all other “unknown unknowns” in the system dynamics. The uncertain model (30.9) constitutes an attempt to embed extra realism into the “ideal” system (30.7). The uncertainties in (30.9) are called “matched,” in the sense that they enter the system dynamics through control channels. So, as long as Λ is invertible, the system controllability property is preserved. It so happens that the matched uncertainty assumption implies

existence of at least one control solution, capable of steering the system state along the desired trajectories.

Of interest are command tracking problems with nonmatched but bounded uncertainties, such as time-dependent noise and environmental disturbances, represented by an n -dimensional uniformly bounded piece-wise continuous vector function $\xi(t)$:

$$\dot{x} = Ax + B\Lambda(u + f(x)) + \xi(t) \quad (30.10)$$

Care must be taken in specifying conditions on $\xi(t)$ that preserve controllability of the system. So as long as the system remains controllable, the unwanted effects caused by bounded noise and disturbances can be mitigated through proper control synthesis. The forthcoming sections explore robust and adaptive methods to control uncertain systems, such as (30.9) and (30.10).

Readers may find the matched uncertainty assumption to be restrictive. Some may even argue that there are many dynamical systems, stemming from realistic applications, that do not satisfy the matching conditions. This is a true statement indeed. However, in aerospace applications, matched uncertainties are of primary concern. They represent unknown aerodynamic and thrust effects that may exist in the vehicle moments. These uncertainties are “matched” by available controls (such as elevator, aileron, rudder, etc.), in the sense that the moments explicitly depend on the control inputs, and the latter can be selected to counter (i.e., cancel or dominate) the matched uncertainties. In essence, moment regulation for an aircraft implies total control of the vehicle, and uncertain dynamical systems in the form of (30.10) can be utilized to achieve that goal. Finally, it is worth noting that the adaptive control methods presented in this chapter can be extended to handle systems with nonlinear-in-control matched uncertainties and with nonmatched uncertain dynamics, but these extensions are outside of the present scope.

30.4 Model Following LQR PI Command Tracking

For a linear time-invariant (LTI) system, such as (30.7), a model following command tracking control design can be defined to represent an LQR-optimal controller, with PI feedback connections. Overall, this design method generalizes the well-known servomechanism approach to a model following design.

Consider an LTI system in the form

$$\begin{aligned} \dot{x}_p &= A_p x_p + B_p u \\ y_p &= C_p x_p + D_p u \end{aligned} \quad (30.11)$$

where $x_p \in R^{n_p}$ is the n_p -dimensional state vector, $u \in R^{m_p}$ is the m_p -dimensional vector of controls, $y_p \in R^{p_p}$ is the system p_p -dimensional vector of regulated outputs with $p_p \leq m_p$, and plant matrices (A_p, B_p, C_p, D_p) are of the corresponding dimensions. Moreover, it is assumed that matrix pair (A_p, B_p) is

stabilizable and the entire state vector x_p is available online as the system output measurement.

The control task of interest is command tracking, that is, one needs to find u such that the regulated output y_p tracks its target $y_{\text{ref}} \in R^{p_p}$, while all other signals in the system remain bounded.

Desired dynamics of the target output y_{ref} is defined via the reference model:

$$\begin{aligned}\dot{x}_{\text{ref}} &= A_{\text{ref}} x_{\text{ref}} + B_{\text{ref}} r(t) \\ y_{\text{ref}} &= C_{\text{ref}} x_{\text{ref}} + D_{\text{ref}} r(t)\end{aligned}\quad (30.12)$$

where $x_{\text{ref}} \in R^{n_{\text{ref}}}$ is the state of the reference dynamics, $r(t)$ represents a bounded external command, and matrices $(A_{\text{ref}}, B_{\text{ref}}, C_{\text{ref}}, D_{\text{ref}})$ are of the corresponding dimensions, with A_{ref} being Hurwitz. Furthermore, it is assumed that the system DC gain matrix is unity, that is

$$DC_{\text{gain}}^{\text{ref}} = -C_{\text{ref}} A_{\text{ref}}^{-1} B_{\text{ref}} + D_{\text{ref}} = I_{m_p \times m_p} \quad (30.13)$$

Note that the dimension of the reference model $n_{\text{ref}} \geq p_p$, and it does not have to be the same as the dimension of the plant n_p .

Extended open-loop dynamics is formed as a combination of the plant and the reference model:

$$\underbrace{\begin{pmatrix} \dot{x}_p \\ \dot{x}_{\text{ref}} \end{pmatrix}}_{\dot{x}} = \underbrace{\begin{pmatrix} A_p & 0_{n_p \times n_{\text{ref}}} \\ 0_{n_{\text{ref}} \times n_p} & A_{\text{ref}} \end{pmatrix}}_A \underbrace{\begin{pmatrix} x_p \\ x_{\text{ref}} \end{pmatrix}}_x + \underbrace{\begin{pmatrix} B_p \\ 0_{n_{\text{ref}} \times m_p} \end{pmatrix}}_B u + \underbrace{\begin{pmatrix} 0_{n_p \times m_p} \\ B_{\text{ref}} \end{pmatrix}}_{B_r} r(t) \quad (30.14)$$

Its regulated output can be written as

$$y = y_p - y_{\text{ref}} = C_p x_p + D_p u - C_{\text{ref}} x_{\text{ref}} - D_{\text{ref}} r(t) \quad (30.15)$$

or, equivalently in matrix form as

$$y = \underbrace{(C_p - C_{\text{ref}})}_C \underbrace{\begin{pmatrix} x_p \\ x_{\text{ref}} \end{pmatrix}}_x + \underbrace{D_p}_D u + \underbrace{(-D_{\text{ref}})}_{D_r} r(t) \quad (30.16)$$

Combining (30.14) and (30.16) yields extended open-loop dynamics in matrix form:

$$\begin{aligned}\dot{x} &= A x + B u + B_r r(t) \\ y &= C x + D u + D_r r(t)\end{aligned}\quad (30.17)$$

Note the explicit presence of the command $r(t)$ in the plant formulation (30.17). This is one way to embed a reference model tracking into the control problem

formulation. Once again, one must choose the reference model data such that the extended system (30.17) remains controllable.

In terms of (30.17), the control task consists of finding u such that the system output y asymptotically tends to the origin. In other words, the control design task is output stabilization in the presence of any known, bounded, and possibly time-varying external command signal $r(t)$.

In order to track a step-input command with zero errors (type-1 response), integral control will be employed. A convenient technique for designing a practical tracker is the command-generator tracker (CGT) method, where the tracking problem is converted into a regulator problem (Franklin et al. 1986). Toward that end, integrated tracking error vector e_{yI} is introduced into the system dynamics (30.17):

$$\begin{aligned} \dot{e}_{yI} &= y \\ \dot{x} &= Ax + Bu + B_r r \\ y &= Cx + Du + D_r r \end{aligned} \quad (30.18)$$

Rewriting the dynamics in matrix form gives

$$\underbrace{\begin{pmatrix} \dot{e}_{yI} \\ \dot{x} \end{pmatrix}}_{\dot{\tilde{x}}} = \underbrace{\begin{pmatrix} 0_{p_p \times p_p} & C \\ 0_{n_p \times p_p} & A \end{pmatrix}}_{\tilde{A}} \underbrace{\begin{pmatrix} e_{yI} \\ x \end{pmatrix}}_{\tilde{x}} + \underbrace{\begin{pmatrix} D_p \\ B \end{pmatrix}}_{\tilde{B}} u + \underbrace{\begin{pmatrix} D_r \\ B_r \end{pmatrix}}_{\tilde{B}_r} r(t) \quad (30.19)$$

with the regulated output defined as

$$y = \underbrace{\begin{pmatrix} 0_{p_p \times p_p} & C \end{pmatrix}}_{\tilde{C}} \underbrace{\begin{pmatrix} e_{yI} \\ x \end{pmatrix}}_{\tilde{x}} + \underbrace{D}_{\tilde{D}} u + \underbrace{D_r}_{\tilde{D}_r} r(t) \quad (30.20)$$

Assuming that the matrix pair (\tilde{A}, \tilde{B}) is controllable, control design for the open-loop dynamics in (30.19) can now be performed using LQR servomechanism approach. Toward that end, assume constant external command $r(t) = r$, utilize matrices as defined in (30.19) and (30.20):

$$\tilde{A} = \begin{pmatrix} 0_{p_p \times p_p} & C \\ 0_{n \times p_p} & A \end{pmatrix}, \quad \tilde{B} = \begin{pmatrix} D \\ B \end{pmatrix}, \quad \tilde{D} = D, \quad \tilde{D}_r = D_r \quad (30.21)$$

and consider stabilization of

$$\dot{z} = \tilde{A}z + \tilde{B}v \quad (30.22)$$

where

$$z = \begin{pmatrix} \dot{e}_{yI} \\ \dot{x} \end{pmatrix}, \quad v = \dot{u} \quad (30.23)$$

It is easy to see that dynamics (30.22) are obtained by differentiating (30.19) while assuming constant external command $r(t) = r$. Next, the newly introduced control

input v in (30.22) is chosen to minimize the LQR performance index (cost):

$$J = \int_0^{\infty} (z^T Q z + v^T R v) dt \tag{30.24}$$

where $Q = Q^T \geq 0$ and $R = R^T > 0$ are the LQR weight matrices. Then, the algebraic Riccati equation

$$\tilde{A}^T P + P \tilde{A} + Q - P \tilde{B} R^{-1} \tilde{B}^T P = 0 \tag{30.25}$$

has a unique positive definite symmetric solution $P = P^T > 0$. Based on the latter, the corresponding LQR-optimal control strategy is given in feedback form:

$$\dot{u} = v = - \underbrace{R^{-1} \tilde{B}^T P}_{K} z = -K z = - (K_I \ K_P) \begin{pmatrix} \dot{e}_{yI} \\ \dot{x} \end{pmatrix} \tag{30.26}$$

Integrating both sides and ignoring constants of integration yields the LQR-optimal control solution in PI feedback form:

$$u = -K_I e_{yI} - K_P x = K_I \frac{(y_{ref} - y)}{s} - K_P x = \boxed{K_I \frac{(y_{ref} - y)}{s} - K_P^x x - K_P^{x_{ref}} x_{ref}} \tag{30.27}$$

where proportional gains K_P^x and $K_P^{x_{ref}}$ are defined below

$$K_P = (K_P^x \ K_P^{x_{ref}}) \tag{30.28}$$

Using LQR feedback (30.27) to control plant dynamics (30.11) will force the system-regulated output y_p to track its command target y_{ref} , which in turn tracks a step-input external command r with zero steady-state error. As a result, the system output y_p will converge to r exponentially fast (for a step input and in steady state). The model following command tracking problem is solved. Figure 30.2 shows the corresponding closed-loop system block-diagram.

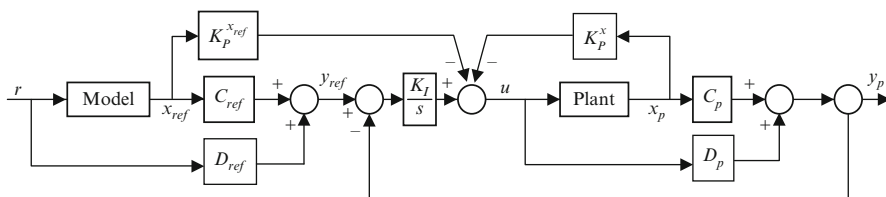
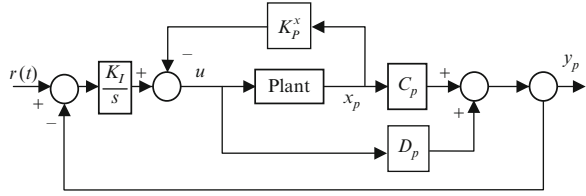


Fig. 30.2 Model following LQR PI control block-diagram

Fig. 30.3 Servomechanism LQR PI control block-diagram



The plant and the model shown in the figure are defined by (30.11) and (30.12), respectively. The reference model dynamics in (30.12) should not be confused with the assumed dynamics of the external command r . Most often, the assumed dynamics is defined as $\dot{r} = 0$, that is, the system is required to track step inputs with zero error. On the other hand, the reference model can be viewed as the command prefilter, that is the system will track the output of the reference model rather than the command itself. Thus, the main purpose of the reference model is to smooth out the command r before it goes into the system, and the model following state feedback LQR PI controller is designed to do precisely that.

If $(A_{\text{ref}}, B_{\text{ref}}, C_{\text{ref}})$ are set to zero and D_{ref} is the identity matrix, then according to (30.12), $y_{\text{ref}} = r(t)$ and the model following architecture from Fig. 30.2 reduces to the standard servomechanism control block-diagram (Fig. 30.3).

Note that in this case, the extended system remains controllable as long as

$$\text{rank} \begin{pmatrix} A_p & B_p \\ C_p & D_p \end{pmatrix} = n_p + m$$

which places restrictions on the regulated output selection.

30.4.1 Design Example: Lateral-Directional LQR PI Control with Explicit Model Following

In order to gain insights into the design, consider the aircraft lateral-directional dynamics (30.6), with the regulated output, whose components are the vehicle roll rate p_s and the angle of sideslip (AOS) β :

$$\underbrace{\begin{pmatrix} \dot{\beta} \\ \dot{p}_s \\ \dot{r}_s \end{pmatrix}}_{\dot{x}_p} = \underbrace{\begin{pmatrix} \frac{Y_\beta}{V_0} & \frac{Y_p}{V_0} & \frac{Y_r}{V_0} - 1 \\ L_\beta & L_p & L_r \\ N_\beta & N_p & N_r \end{pmatrix}}_{A_p} \underbrace{\begin{pmatrix} \beta \\ p_s \\ r_s \end{pmatrix}}_{x_p} + \underbrace{\begin{pmatrix} \frac{Y_{\delta_a}}{V_0} & \frac{Y_{\delta_r}}{V_0} \\ L_{\delta_a} & L_{\delta_r} \\ N_{\delta_a} & N_{\delta_r} \end{pmatrix}}_{B_p} \underbrace{\begin{pmatrix} \delta_{\text{ail}} \\ \delta_{\text{rud}} \end{pmatrix}}_u \tag{30.29}$$

$$y_p = \begin{pmatrix} p_s \\ \beta \end{pmatrix} = \underbrace{\begin{pmatrix} 0 & 1 & 0 \\ 1 & 0 & 0 \end{pmatrix}}_{C_p} x_p + \underbrace{0_{2 \times 2}}_{D_p} u$$

where (p_s, r_s) are the aircraft roll and yaw angular rates in stability axes, $(\delta_{\text{ail}}, \delta_{\text{rud}})$ are the control inputs (aileron and rudder deflections), and V_0 is the aircraft true airspeed (trimmed). The rest of the parameters in the model represent the vehicle stability and control derivatives. In (30.29), $n_p = 3$, $m_p = p_p = 2$.

The control task is to construct aileron δ_{ail} and rudder δ_{rud} such that the aircraft roll rate p_s and AOS β track their step-input commands, p_{cmd} and β_{cmd} , respectively, while all other signals in the system remain bounded.

Desired roll rate and AOS dynamics are defined by the LTI reference model:

$$\begin{aligned} \underbrace{\begin{pmatrix} \dot{p}_{\text{ref}} \\ \dot{\beta}_{\text{ref}} \end{pmatrix}}_{\dot{x}_{\text{ref}}} &= \underbrace{\begin{pmatrix} -\frac{1}{\tau_p} & 0 \\ 0 & -\frac{1}{\tau_\beta} \end{pmatrix}}_{A_{\text{ref}}} \underbrace{\begin{pmatrix} p_{\text{ref}} \\ \beta_{\text{ref}} \end{pmatrix}}_{x_{\text{ref}}} + \underbrace{\begin{pmatrix} \frac{1}{\tau_p} & 0 \\ 0 & \frac{1}{\tau_\beta} \end{pmatrix}}_{B_{\text{ref}}} \underbrace{\begin{pmatrix} p_{\text{cmd}} \\ \beta_{\text{cmd}} \end{pmatrix}}_{r(t)} \\ y_{\text{ref}} &= \underbrace{\begin{pmatrix} 1 & 0 \\ 0 & 1 \end{pmatrix}}_{C_{\text{ref}}} x_{\text{ref}} + \underbrace{0_{2 \times 2}}_{D_{\text{ref}}} r(t) \end{aligned} \quad (30.30)$$

where τ_p and τ_β are small positive time constants that define the desired roll rate and the AOS dynamics, correspondingly. It is easy to check that the DC gain of the reference model is unity.

From (30.29) and (30.30) it follows that

$$n_p = 3, \quad p_p = m_p = 2, \quad n_{\text{ref}} = 2 \quad (30.31)$$

Using (30.14) gives extended open-loop dynamics:

$$\underbrace{\begin{pmatrix} \dot{x}_p \\ \dot{x}_{\text{ref}} \end{pmatrix}}_{\dot{x}} = \underbrace{\begin{pmatrix} A_p & 0_{3 \times 2} \\ 0_{2 \times 3} & A_{\text{ref}} \end{pmatrix}}_A \underbrace{\begin{pmatrix} x_p \\ x_{\text{ref}} \end{pmatrix}}_x + \underbrace{\begin{pmatrix} B_p \\ 0_{2 \times 2} \end{pmatrix}}_B \underbrace{\begin{pmatrix} \delta_{\text{ail}} \\ \delta_{\text{rud}} \end{pmatrix}}_u + \underbrace{\begin{pmatrix} 0_{3 \times 2} \\ B_{\text{ref}} \end{pmatrix}}_{B_r} \underbrace{\begin{pmatrix} p_{\text{cmd}} \\ \beta_{\text{cmd}} \end{pmatrix}}_{r(t)} \quad (30.32)$$

where matrix pairs (A_p, B_p) and $(A_{\text{ref}}, B_{\text{ref}})$ are as in (30.29) and (30.30). According to (30.15), the system-regulated output is

$$y = y_p - y_{\text{ref}} = C_p x_p - C_{\text{ref}} x_{\text{ref}} = \underbrace{(C_p - C_{\text{ref}})}_C x + \underbrace{0_{2 \times 2}}_D u + \underbrace{0_{2 \times 2}}_{D_r} r(t) \quad (30.33)$$

Per (30.18), the extended dynamics (30.32) are augmented with the roll rate and AOS integrated tracking errors:

$$\begin{aligned} \dot{e}_{pI} &= p - p_{\text{ref}} \\ \dot{e}_{\beta I} &= \beta - \beta_{\text{ref}} \\ \dot{x} &= A x + B u + B_r r(t) \\ y &= C x \end{aligned} \quad (30.34)$$

The integrated tracking error vector e_{yI} has two components: integrated roll rate error e_{pI} and integrated AOS error $e_{\beta I}$. Similar to (30.19), one gets

$$\underbrace{\begin{pmatrix} \dot{e}_{yI} \\ \dot{x} \end{pmatrix}}_{\ddot{x}} = \underbrace{\begin{pmatrix} 0_{2 \times 2} & C \\ 0_{5 \times 2} & A \end{pmatrix}}_{\tilde{A}} \underbrace{\begin{pmatrix} e_{yI} \\ x \end{pmatrix}}_{\tilde{x}} + \underbrace{\begin{pmatrix} 0_{2 \times 2} \\ B \end{pmatrix}}_{\tilde{B}} u + \underbrace{\begin{pmatrix} 0_{2 \times 2} \\ B_r \end{pmatrix}}_{\tilde{B}_r} r(t) \quad (30.35)$$

with the regulated output as in (30.20).

$$y = \begin{pmatrix} p - p_{\text{ref}} \\ \beta - \beta_{\text{ref}} \end{pmatrix} = \underbrace{\begin{pmatrix} 0_{2 \times 2} & C \end{pmatrix}}_{\tilde{c}} \tilde{x} + \underbrace{0_{m_p \times m_p}}_{\tilde{d}} u + \underbrace{0_{m_p \times m_p}}_{\tilde{d}_r} r(t) \quad (30.36)$$

Using matrices (\tilde{A}, \tilde{B}) from (30.35), choosing LQR weights (Q, R) appropriately, and solving the algebraic Riccati equation (30.25), yields the LQR PI matrix of optimal gains (see (30.26)):

$$K = R^{-1} \tilde{B}^T P \quad (30.37)$$

Partitioning the gains as in (30.28), the LQR-optimal control solution can be written in the form of (30.27):

$$u = K_I \frac{(y_{\text{ref}} - y)}{s} - K_P^x x - K_P^{x_{\text{ref}}} x_{\text{ref}} \quad (30.38)$$

where

$$K = \left(K_I \quad K_P^x \quad K_P^{x_{\text{ref}}} \right) \quad (30.39)$$

In terms of the original notation, the model following LQR PI controller can be expressed as

$$\begin{cases} \delta_{\text{ail}} = K_{pI}^{\text{ail}} \frac{(p_{\text{ref}} - p)}{s} + K_{\beta I}^{\text{ail}} \frac{(\beta_{\text{ref}} - \beta)}{s} - K_{\beta}^{\text{ail}} \beta - K_p^{\text{ail}} p_s - K_r^{\text{ail}} r_s - K_{p_{\text{ref}}}^{\text{ail}} p_{\text{ref}} - K_{\beta_{\text{ref}}}^{\text{ail}} \beta_{\text{ref}} \\ \delta_{\text{rud}} = K_{pI}^{\text{rud}} \frac{(p_{\text{ref}} - p)}{s} + K_{\beta I}^{\text{rud}} \frac{(\beta_{\text{ref}} - \beta)}{s} - K_{\beta}^{\text{rud}} \beta - K_p^{\text{rud}} p_s - K_r^{\text{rud}} r_s - K_{p_{\text{ref}}}^{\text{rud}} p_{\text{ref}} - K_{\beta_{\text{ref}}}^{\text{rud}} \beta_{\text{ref}} \end{cases} \quad (30.40)$$

Comparing (30.39) and (30.40), yields the LQR PI optimal matrix gains:

$$K_I = \begin{pmatrix} K_{pI}^{\text{ail}} & K_{\beta I}^{\text{ail}} \\ K_{pI}^{\text{rud}} & K_{\beta I}^{\text{rud}} \end{pmatrix}, \quad K_P^x = \begin{pmatrix} K_{\beta}^{\text{ail}} & K_p^{\text{ail}} & K_r^{\text{ail}} \\ K_{\beta}^{\text{rud}} & K_p^{\text{rud}} & K_r^{\text{rud}} \end{pmatrix}, \quad K_P^{x_{\text{ref}}} = \begin{pmatrix} K_{p_{\text{ref}}}^{\text{ail}} & K_{\beta_{\text{ref}}}^{\text{ail}} \\ K_{p_{\text{ref}}}^{\text{rud}} & K_{\beta_{\text{ref}}}^{\text{rud}} \end{pmatrix} \quad (30.41)$$

The reader is encouraged to test this technique on a specific system of choice. Although the controller was designed to track step-input commands, its command following performance will be excellent for any bounded command, whose rate of change is within the closed-loop system bandwidth. In addition, one can and should

compute stability margins, at the plant input and output break points. These margins will be excessive, which is to be expected for any LQR-based design. In addition, the closed-loop system will be robust due to a large class of state-dependent nonlinear uncertainties (matched), confined within a sector, that may exist at the plant input. All these features make the LQR PI feedback design highly efficient in controlling aerial platforms. The next section introduces adaptive augmentation algorithms to extend robustness of an LQR PI controller, with respect to a wide class of matched uncertainties and beyond.

30.5 Model Reference Adaptive Control

The concept of model reference adaptive control (MRAC) was originally proposed in 1958 by Whitaker et al., at MIT (Whitaker et al. 1958), and later extended in (Butchart and Shackcloth 1965; Parks 1966). Current state of the art in adaptive control is well documented and can be found in textbooks (Narendra and Annaswamy 2005; Ioannou and Fidan 2006). The original intent of adaptive control was to specify the desired command-to-output performance of a servo-tracking system using a reference model that would define the ideal response of the system due to external commands. A generic block-diagram of the MRAC system is shown in Fig. 30.4.

As seen from the diagram, the controller parameter adjustments (the adaptive law) are made based on the tracking error (the difference between the system actual response and its target specified by the reference model output), an output feedback from the process, and the external command. For the sake of clarity and in order to motivate further discussions, consider MRAC design equations for a scalar system shown below:

$$\begin{array}{l}
 \text{Process : } \dot{x} = ax + bu \\
 \text{Ref. Model : } \dot{x}_{\text{ref}} = a_{\text{ref}}x_{\text{ref}} + b_{\text{ref}}r \\
 \text{Controller : } u = \hat{k}_x x + \hat{k}_r r \\
 \text{Adaptive Law : } \begin{cases} \hat{k}_x = -\gamma_x x (x - x_{\text{ref}}) \\ \hat{k}_r = -\gamma_r r (x - x_{\text{ref}}) \end{cases}
 \end{array} \tag{30.42}$$

where a and b are unknown constant parameters in the process dynamics with the known $sgnb > 0$. The control input u is selected such that the system state x follows the reference model state x_{ref} , driven by any bounded external command $r = r(t)$. Also in (30.42), the reference model data $a_{\text{ref}} < 0$ and b_{ref} are chosen to yield the desired speed of response and a DC gain (unity in most applications) from the reference model output $y_{\text{ref}} = x_{\text{ref}}$ to the system-regulated output $y = x$.

In this case, closed-loop system stability and global asymptotic tracking are achieved via a specific choice of the adaptive law in (30.42), with the adaptive

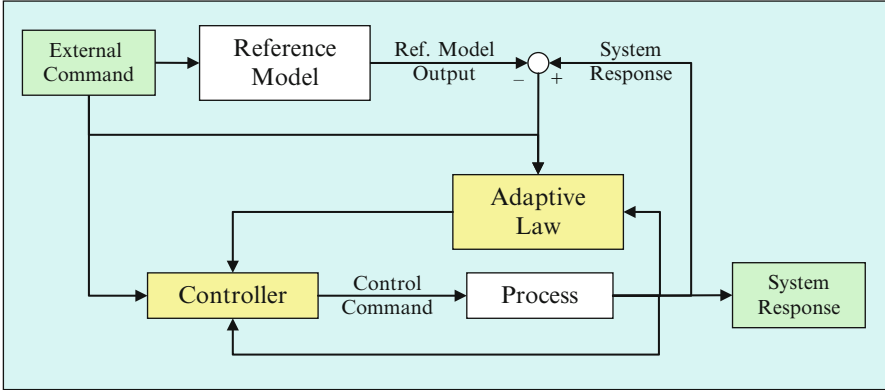


Fig. 30.4 MRAC block-diagram

gains (\hat{k}_x, \hat{k}_r) , whose dynamics are influenced by two positive constant rates of adaptation (γ_x, γ_r) . As seen from (30.42), the state tracking error

$$e = x - x_{ref} \tag{30.43}$$

drives the adaptive laws. Existence of a servo-control solution for this particular scalar dynamics is provided by the matching conditions:

$$\begin{aligned} a_{ref} &= a + b k_x \\ b_{ref} &= b k_r \end{aligned} \tag{30.44}$$

where k_x and k_r denote the ideal unknown constant parameters (gains of the ideal controller). For scalar dynamics, such as the process in (30.42), it is clear that the matching relations (30.44) always have a solution. Let,

$$\Delta k_x = \hat{k}_x - k_x, \quad \Delta k_r = \hat{k}_r - k_r \tag{30.45}$$

represent the parameter estimation errors. Substituting the matching conditions (30.44) into (30.42), one can derive the tracking error dynamics:

$$\dot{e} = a_{ref} e + b (\Delta k_x x + \Delta k_r r) \tag{30.46}$$

which indeed define transients in the corresponding closed-loop system. The tracking error dynamics and the transient dynamics are equivalent notions. If and when e becomes small (asymptotically), the system output tracks the reference model with diminishing errors. On the other hand, the transient dynamics define what happens between the start of a maneuver and the time when the error gets small. Both questions will be addressed next.

Going back to (30.46), one can employ Lyapunov arguments (Khalil 1996) to prove global asymptotic stability of the tracking error dynamics. In fact, using a radially unbounded quadratic Lyapunov function candidate in the form

$$V(e, \Delta k_x, \Delta k_r) = e^2 + \left(\frac{\Delta k_x^2}{\gamma_x} + \frac{\Delta k_r^2}{\gamma_r} \right) * b \quad (30.47)$$

it is not difficult to show that with the adaptive law (30.42), the time derivative of V , evaluated along the trajectories of the error dynamics (30.46), becomes nonpositive. This argument constitutes the inverse Lyapunov-based design. It provides (a) the adaptive law and (b) the required proof of closed-loop global asymptotic stability. As a result, one can formally show that for any initial condition, any bounded time-varying external command, and any positive rates of adaptation, the tracking error dynamics (30.46) are globally asymptotically stable:

$$\lim_{t \rightarrow \infty} |e(t)| = \lim_{t \rightarrow \infty} |x(t) - x_{\text{ref}}(t)| = 0 \quad (30.48)$$

and all signals in the corresponding closed-loop dynamics remain uniformly bounded, forward in time.

30.5.1 MRAC Design for MIMO Dynamics

The scalar MRAC design methodology generalizes to multi-input-multi-output (MIMO) systems with matched parametric uncertainties in the form

$$\dot{x} = Ax + B\Lambda(u + f(x)) \quad (30.49)$$

where $x \in R^n$ is the system state, $u \in R^m$ is the control input, and $B \in R^{n \times m}$ is the known control matrix, while $A \in R^{n \times n}$ and $\Lambda \in R^{m \times m}$ are unknown constant matrices. In addition, it is assumed that Λ is diagonal, its elements λ_i are strictly positive, and the pair $(A, B\Lambda)$ is controllable. The uncertainty in Λ is introduced to model control effectiveness failures or modeling errors. In (30.49), the unknown possibly nonlinear vector function $f(x) : R^n \rightarrow R^m$ represents the system-matched uncertainty. It is assumed that each individual component $f_i(x)$ of $f(x)$ can be written as a linear combination of N known locally Lipschitz-continuous basis functions $\phi_i(x)$, with unknown constant coefficients. So,

$$f(x) = \Theta^T \Phi(x) \quad (30.50)$$

where $\Theta \in R^{N \times m}$ is a constant matrix of the unknown coefficients and

$$\Phi(x) = (\phi_1(x) \dots \phi_N(x))^T \in R^N$$

is the known regressor vector. Of interest is the design of a MIMO state feedback adaptive control law such that the system state x globally uniformly asymptotically tracks the state $x_{\text{ref}} \in R^n$ of the reference model

$$\dot{x}_{\text{ref}} = A_{\text{ref}} x_{\text{ref}} + B_{\text{ref}} r(t) \quad (30.51)$$

where $A_{\text{ref}} \in R^{n \times n}$ is Hurwitz, $B_{\text{ref}} \in R^{n \times m}$, and $r(t) \in R^m$ is the external bounded command vector.

It is also required that during tracking, all signals in the closed-loop system remain uniformly bounded. Thus, given any bounded command $r(t)$, the control input u needs to be chosen such that the state tracking error

$$e(t) = x(t) - x_{\text{ref}}(t) \quad (30.52)$$

globally uniformly asymptotically tends to zero, that is,

$$\lim_{t \rightarrow \infty} \|x(t) - x_{\text{ref}}(t)\| = 0 \quad (30.53)$$

If matrices A and Λ were known, one could have calculated and applied the ideal fixed-gain control law:

$$u = K_x^T x + K_r^T r - \Theta^T \Phi(x) \quad (30.54)$$

and obtain the closed-loop system:

$$\dot{x} = (A + B \Lambda K_x^T) x + B \Lambda K_r^T r \quad (30.55)$$

Comparing (30.55) with the desired reference dynamics (30.51), it follows that for the existence of a controller in the form of (30.54), the ideal unknown control gains, K_x and K_r , must satisfy the matching conditions:

$$\begin{aligned} A + B \Lambda K_x^T &= A_{\text{ref}} \\ B \Lambda K_r^T &= B_{\text{ref}} \end{aligned} \quad (30.56)$$

Assuming that these matching conditions hold, it is easy to see that using (30.54) yields the closed-loop system which is exactly the same as the reference model. Consequently, for any bounded reference input signal $r(t)$, the fixed-gain controller (30.54) provides global uniform asymptotic tracking performance. Note that given a set of matrices $(A, B, \Lambda, A_{\text{ref}}, B_{\text{ref}})$, in general there is no guarantee that ideal gains K_x, K_r exist to enforce the matching conditions (30.56). In other words, the control law (30.54) may not be able to meet the design objective. However often in practice, the structure of A is known, and the reference model matrices $A_{\text{ref}}, B_{\text{ref}}$

are chosen so that the system (30.56) has at least one ideal solution pair (K_x, K_r) . Assuming that K_x, K_r in (30.56) do exist, consider the following control law:

$$u = \hat{K}_x^T x + \hat{K}_r^T r - \hat{\Theta}^T \Phi(x) \quad (30.57)$$

where $\hat{K}_x \in R^{n \times m}$, $\hat{K}_r \in R^{m \times m}$, $\hat{\Theta} \in R^{N \times n}$ are the estimates of the ideal unknown matrices K_x, K_r, Θ , respectively. These estimated parameters will be generated online through the inverse Lyapunov analysis. Substituting (30.57) into (30.49), the closed-loop system dynamics can be written as

$$\dot{x} = \left(A + B \Lambda \hat{K}_x^T \right) x + B \Lambda \left(\hat{K}_r^T r - \left(\hat{\Theta} - \Theta \right)^T \Phi(x) \right) \quad (30.58)$$

Subtracting (30.51) from (30.58), it is possible to compute the closed-loop dynamics of the n -dimensional tracking error vector $e(t) = x(t) - x_{\text{ref}}(t)$:

$$\dot{e} = \left(A + B \Lambda \hat{K}_x^T \right) x + B \Lambda \left(\hat{K}_r^T r - \left(\hat{\Theta} - \Theta \right)^T \Phi(x) \right) - A_{\text{ref}} x_{\text{ref}} - B_{\text{ref}} r \quad (30.59)$$

With the matching conditions (30.56) in place, one further gets

$$\begin{aligned} \dot{e} &= \left(A_{\text{ref}} + B \Lambda \left(\hat{K}_x - K_x \right) \right) x - A_{\text{ref}} x_{\text{ref}} + B \Lambda \left(\hat{K}_r - K_r \right) r - B \Lambda \\ &\quad \left(\hat{\Theta} - \Theta \right)^T \Phi(x) \\ &= A_{\text{ref}} e + B \Lambda \left[\left(\hat{K}_x - K_x \right)^T x + \left(\hat{K}_r - K_r \right)^T r - \left(\hat{\Theta} - \Theta \right)^T \Phi(x) \right] \end{aligned} \quad (30.60)$$

Let $\Delta K_x = \hat{K}_x - K_x$, $\Delta K_r = \hat{K}_r - K_r$, and $\Delta \Theta = \hat{\Theta} - \Theta$ represent the parameter estimation errors. In terms of the latter, the tracking error dynamics become

$$\dot{e} = A_{\text{ref}} e + B \Lambda \left[\Delta K_x^T x + \Delta K_r^T r - \Delta \Theta^T \Phi(x) \right] \quad (30.61)$$

Introduce rates of adaptation: $\Gamma_x = \Gamma_x^T > 0$, $\Gamma_r = \Gamma_r^T > 0$, $\Gamma_\Theta = \Gamma_\Theta^T > 0$. Going back to analyzing stability of the tracking error dynamics (30.61), consider a globally radially unbounded quadratic Lyapunov function candidate in the form

$$\begin{aligned} V(e, \Delta K_x, \Delta K_r, \Delta \Theta) &= e^T P e + \text{tr} \left(\left[\Delta K_x^T \Gamma_x^{-1} \Delta K_x + \Delta K_r^T \Gamma_r^{-1} \Delta K_r \right. \right. \\ &\quad \left. \left. + \Delta \Theta^T \Gamma_\Theta^{-1} \Delta \Theta \right] \Lambda \right) \end{aligned} \quad (30.62)$$

where $P = P^T > 0$ satisfies the algebraic Lyapunov equation

$$P A_{\text{ref}} + A_{\text{ref}}^T P = -Q \quad (30.63)$$

for some $Q = Q^T > 0$. Then the time derivative of V , evaluated along the trajectories of (30.61), can be calculated:

$$\begin{aligned}
 \dot{V} &= \dot{e}^T P e + e^T P \dot{e} + 2 \operatorname{tr} \left(\left[\Delta K_x^T \Gamma_x^{-1} \dot{\hat{K}}_x + \Delta K_r^T \Gamma_r^{-1} \dot{\hat{K}}_r + \Delta \Theta^T \Gamma_\Theta^{-1} \dot{\hat{\Theta}} \right] \Lambda \right) \\
 &= (A_{\text{ref}} e + B \Lambda (\Delta K_x^T x + \Delta K_r^T r - \Delta \Theta^T \Phi(x)))^T P e \\
 &\quad + e^T P (A_{\text{ref}} e + B \Lambda (\Delta K_x^T x + \Delta K_r^T r - \Delta \Theta^T \Phi(x))) \\
 &\quad + 2 \operatorname{tr} \left(\left[\Delta K_x^T \Gamma_x^{-1} \dot{\hat{K}}_x + \Delta K_r^T \Gamma_r^{-1} \dot{\hat{K}}_r + \Delta \Theta^T \Gamma_\Theta^{-1} \dot{\hat{\Theta}} \right] \Lambda \right) \\
 &= e^T (A_{\text{ref}} P + P A_{\text{ref}}) e + 2 e^T P B \Lambda (\Delta K_x^T x + \Delta K_r^T r - \Delta \Theta^T \Phi(x)) \\
 &\quad + 2 \operatorname{tr} \left(\left[\Delta K_x^T \Gamma_x^{-1} \dot{\hat{K}}_x + \Delta K_r^T \Gamma_r^{-1} \dot{\hat{K}}_r + \Delta \Theta^T \Gamma_\Theta^{-1} \dot{\hat{\Theta}} \right] \Lambda \right) \quad (30.64)
 \end{aligned}$$

Using (30.63) further yields

$$\begin{aligned}
 \dot{V} &= -e^T Q e + \left[2 e^T P B \Lambda \Delta K_x^T x + 2 \operatorname{tr} \left(\Delta K_x^T \Gamma_x^{-1} \dot{\hat{K}}_x \Lambda \right) \right] \\
 &\quad + \left[2 e^T P B \Lambda \Delta K_r^T r + 2 \operatorname{tr} \left(\Delta K_r^T \Gamma_r^{-1} \dot{\hat{K}}_r \Lambda \right) \right] \\
 &\quad + \left[-2 e^T P B \Lambda \Delta \Theta^T \Phi(x) + 2 \operatorname{tr} \left(\Delta \Theta^T \Gamma_\Theta^{-1} \dot{\hat{\Theta}} \Lambda \right) \right] \quad (30.65)
 \end{aligned}$$

Via the well-known trace identity

$$\begin{aligned}
 \underbrace{e^T P B \Lambda}_{a^T} \underbrace{\Delta K_x^T x}_b &= \operatorname{tr} \left(\underbrace{\Delta K_x^T x}_b \underbrace{e^T P B \Lambda}_{a^T} \right) \\
 \underbrace{e^T P B \Lambda}_{a^T} \underbrace{\Delta K_r^T r}_b &= \operatorname{tr} \left(\underbrace{\Delta K_r^T r}_b \underbrace{e^T P B \Lambda}_{a^T} \right) \\
 \underbrace{e^T P B \Lambda}_{a^T} \underbrace{\Delta \Theta^T \Phi(x)}_b &= \operatorname{tr} \left(\underbrace{\Delta \Theta^T \Phi(x)}_b \underbrace{e^T P B \Lambda}_{a^T} \right)
 \end{aligned} \quad (30.66)$$

Substituting (30.66) into (30.65) results in

$$\begin{aligned}
 \dot{V} &= -e^T Q e + 2 \operatorname{tr} \left(\Delta K_x^T \left[\Gamma_x^{-1} \dot{\hat{K}}_x + x e^T P B \right] \Lambda \right) \\
 &\quad + 2 \operatorname{tr} \left(\Delta K_r^T \left[\Gamma_r^{-1} \dot{\hat{K}}_r + r e^T P B \right] \Lambda \right) + 2 \operatorname{tr} \left(\Delta \Theta^T \left[\Gamma_\Theta^{-1} \dot{\hat{\Theta}} - \Phi(x) e^T P B \right] \Lambda \right) \quad (30.67)
 \end{aligned}$$

If the adaptive laws are selected as

$$\begin{aligned}\dot{\hat{K}}_x &= -\Gamma_x x e^T P B \\ \dot{\hat{K}}_r &= -\Gamma_r r(t) e^T P B \\ \dot{\hat{\Theta}} &= \Gamma_\Theta \Phi(x) e^T P B\end{aligned}\quad (30.68)$$

then the time derivative of V in (30.67) becomes globally negative semidefinite:

$$\dot{V} = -e^T Q e \leq 0 \quad (30.69)$$

Therefore, the closed-loop error dynamics are uniformly stable. Hence, the tracking error $e(t)$ as well as the parameter estimation errors $\Delta K_x(t)$, $\Delta K_r(t)$, and $\Delta \Theta(t)$ are uniformly bounded and so are the parameter estimates $\hat{K}_x(t)$, $\hat{K}_r(t)$, and $\hat{\Theta}(t)$. Since $r(t)$ is bounded and A_{ref} is Hurwitz, then $x_{\text{ref}}(t)$ and $\dot{x}_{\text{ref}}(t)$ are bounded. Consequently, the system state $x(t)$ is uniformly bounded, and the control input $u(t)$ in (30.57) is bounded as well. The latter implies that $\dot{x}(t)$ is bounded, and thus $\dot{e}(t)$ is bounded. Furthermore, the second time derivative of $V(t)$

$$\ddot{V} = -e^T Q \dot{e} = -2e^T Q \dot{e} \quad (30.70)$$

is bounded, and so $\dot{V}(t)$ is uniformly continuous. Since in addition, $V(t)$ is lower bounded and $\dot{V}(t) \leq 0$, then using Barbalat's lemma (Khalil 1996) gives $\lim_{t \rightarrow \infty} \dot{V}(t) = 0$, which implies (via (30.69))

$$\left[\lim_{t \rightarrow \infty} e^T Q e = 0 \right] \Leftrightarrow \left[\lim_{t \rightarrow \infty} \|e\| = 0 \right] \Leftrightarrow \left[\lim_{t \rightarrow \infty} \|x(t) - x_{\text{ref}}(t)\| = 0 \right] \quad (30.71)$$

It has been formally proven that the state tracking error $e(t)$ tends to the origin globally, uniformly, and asymptotically. The MIMO command tracking problem is solved, and a summary of the derived MRAC design equations is given in Table 30.1.

30.5.2 MRAC Design Modifications for Robustness

Shown in Table 30.1, the design is valid for MIMO dynamics (30.9), with a positive definite diagonal matrix Λ (control uncertainty) and a matched unknown-in-parameters function $f(x) = \Theta^T \Phi(x)$, where $\Theta \in R^{N \times m}$ represents a constant matrix of unknown parameters, $\Phi(x) \in R^N$ is the known regressor vector, and N is an integer. If components of the regressor are chosen from a certain class of approximation-capable maps (such as splines, trigonometric functions, polynomials, Gaussians, radial basis functions, sigmoidal/ridge functions), then the MIMO adaptive laws will provide semiglobal stability and command tracking for a wide class of matched uncertain functions $f(x)$ and bounded noise $\xi(t)$.

Table 30.1 MIMO MRAC laws

Open-loop plant	$\dot{x} = A x + B \Lambda (u + \Theta^T \Phi(x))$
Reference model	$\dot{x}_{\text{ref}} = A_{\text{ref}} x_{\text{ref}} + B_{\text{ref}} r$
Model matching conditions	$A + B \Lambda K_x^T = A_{\text{ref}}, \quad B \Lambda K_r^T = B_{\text{ref}}$
Tracking error	$e = x - x_{\text{ref}}$
Control input	$u = \hat{K}_x^T x + \hat{K}_r^T r - \hat{\Theta}^T \Phi(x)$
Algebraic Lyapunov equation	$P A_{\text{ref}} + A_{\text{ref}}^T P = -Q$
MIMO MRAC laws	$\begin{aligned} \dot{\hat{K}}_x &= -\Gamma_x x e^T P B \\ \dot{\hat{K}}_r &= -\Gamma_r r(t) e^T P B \\ \dot{\hat{\Theta}} &= \Gamma_{\Theta} \Phi(x) e^T P B \end{aligned}$

Table 30.2 Robustness modifications in MRAC design

Dead-zone	$\dot{\hat{\Theta}} = \Gamma_{\Theta} \Phi(x) \mu(\ e\) e^T P B$
σ -mod	$\dot{\hat{\Theta}} = \Gamma_{\Theta} (\Phi(x) e^T P B - \sigma \hat{\Theta})$
e mod	$\dot{\hat{\Theta}} = \Gamma_{\Theta} (\Phi(x) e^T P B - \sigma \ e^T P B\ \hat{\Theta})$
Projection operator	$\dot{\hat{\Theta}} = \text{Proj}(\hat{\Theta}, \Gamma_{\Theta} \Phi e^T P B)$

These are nonparametric uncertainties. In order to mitigate the latter, the adaptive laws must be modified to become robust (Ioannou and Fidan 2006; Narendra and Annaswamy 2005). Table 30.2 shows four robustness modifications for adaptive control of MIMO uncertain systems, with their dynamics extended to include integrated tracking errors.

Overall, an MRAC controller enforces global uniform asymptotic tracking performance of the preselected reference model dynamics, driven by a bounded time-varying command while keeping the rest of the signals in the corresponding closed-loop system uniformly bounded. Such a controller adapts to matched uncertainties, and it remains robust to nonparametric nonmatched time-varying process noise $\xi(t)$. The key feature that enables robustness of MRAC to process noise is the dead-zone modification (Fig. 30.5):

$$\mu(\|e\|) = \max\left(0, \min\left(1, \frac{\|e\| - \delta e_0}{(1 - \delta) e_0}\right)\right) \tag{30.72}$$

where $0 < \delta < 1$ is a constant.

The dead zone freezes the MRAC laws if and when the magnitude (2-norm) of the tracking error vector

$$e = x - x_{\text{ref}}$$

becomes smaller than a preset tolerance e_0 . Any realistic adaptive system must have a continuous dead-zone modification, such as (30.72), to avoid potential discontinuities in feedback connections. The “must-have” dead-zone modification will prevent adaptive parameters from drifting away due to persisting noise or other nonparametric uncertainties in the system dynamics.

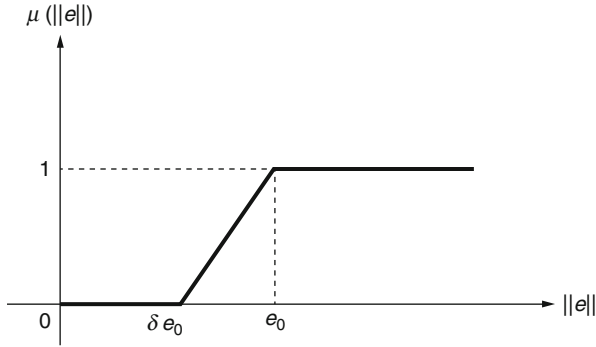


Fig. 30.5 The dead-zone function

Table 30.3 The projection operator

Max parameter bounds	$\ \theta\ \leq \theta^{\max}$
Convex function	$f(\hat{\theta}) = \frac{(1+\varepsilon)\ \hat{\theta}\ ^2 - (\theta^{\max})^2}{\varepsilon(\theta^{\max})^2}$
Two convex sets	$\Omega_0 = \{\theta : f(\theta) \leq 0\} = \{\theta : \ \theta\ \leq \frac{\theta^{\max}}{\sqrt{1+\varepsilon}}\}$ $\Omega_1 = \{\theta : f(\theta) \leq 1\} = \{\theta : \ \theta\ \leq \theta^{\max}\}$
Projection operator	$\text{Proj}(\theta, y) = \begin{cases} y - \frac{\Gamma \nabla f(\theta) (\nabla f(\theta))^T}{(\nabla f(\theta))^T \Gamma \nabla f(\theta)} y f(\theta), & \text{if } [f(\theta) > 0 \wedge (y^T \nabla f(\theta)) > 0] \\ y, & \text{if not} \end{cases}$
Convex inequality for proof of stability	$(\theta - \theta^*)^T (\Gamma^{-1} \text{Proj}(\theta, \Gamma y) - y) \leq 0,$ $\forall \theta^* \in \Omega_0, \theta \in \Omega_1, y \in R^n$
Uniform boundedness of parameters	$\dot{\theta} = \text{Proj}(\theta, \Gamma y)$ $[\theta(0) \in \Omega_0] \Rightarrow [\theta(t) \in \Omega_1, \forall t \geq 0]$

Also of key importance is the projection operator modification (Ioannou and Fidan 2006), shown in Table 30.3.

As defined, this modification acts on two column vectors $(\theta, \Gamma y)$. For matrices, the projection operator is applied column-wise. By design, projection-based MRAC laws will force the tracking error to become small while keeping the adaptive parameters within their prespecified bounds.

Without robustness modifications, the adaptive law dynamics are defined by integrating a nonlinear function, represented by the regressor vector $\Phi(x)$, multiplied by a linear combination of the state tracking errors $(e^T P B)$. This product is further multiplied by a constant matrix Γ_Θ (the integral gain), and finally it is integrated to yield the adaptive parameters $\hat{\Theta}(t)$ (see Fig. 30.6).

As seen from the block-diagram, there is a chain of nonlinear integrators in a feedback loop, whose output constitute the adaptive parameters. In all practical applications, feedback integrators must be “managed” in the sense that their

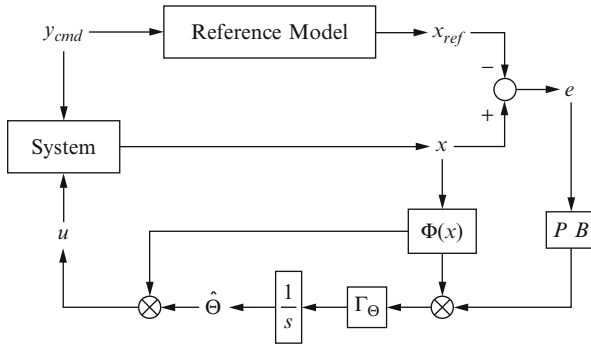


Fig. 30.6 MRAC system viewed as a nonlinear integral feedback controller

output signals (i.e., the adaptive parameters) need to be constrained. This prevents integrators against “winding up” due to nonlinear saturation functions in the control channels, where the system achievable control limits are defined and enforced. Control techniques that prevent the integrator windup problems are called the “anti-windup” methods, and the projection operator is one of them. So in practice, an MRAC architecture would consist of the smoothed dead-zone modification coupled with the projection operator. These are the two must-have modifications for enabling MRAC systems to efficiently operate in unknown environment.

30.5.3 Observer-Based MRAC Design with Transient Guarantees

Even though an adaptive controller enables command tracking asymptotically in time (as $t \rightarrow \infty$), it provides no uniformly guaranteed bounds on how large the transients might become prior to acquiring the command. In order to yield fast tracking and thus shorten transients, one needs to increase the rates of adaptation and, thus, to speed up MRAC laws. However, experience shows that if these rates grow large, unwanted transient oscillations will appear during the initial few seconds (the transient time) of operation. The balance between achieving fast tracking and avoiding undesired transients constitutes the MRAC design trade-off phenomenon. In essence, the rates of adaptation must be chosen large enough for fast tracking but not too large so that unwanted transients are precluded.

To understand the intricacies in MRAC design, reconsider the scalar design (30.42). What complicates the MRAC tuning process is the direct dependence of the transient dynamics (30.46) on (a) the external command and (b) the initial conditions for the system and the adaptive controller. These dependencies may too lead to undesirable transients. Consider the error dynamics (30.46). Using Lyapunov arguments, one can prove that the time-varying signal

$$\varphi(t) = b(\Delta k_x(t) x(t) + \Delta k_r(t) r(t)) \tag{30.73}$$

is uniformly bounded in time and that the tracking error $e(t)$ globally asymptotically tends to zero, as shown in (30.48). Still, the time constant of the transient dynamics (30.46) $\tau_e = \frac{1}{|a_{\text{ref}}|}$ is exactly the same as in the reference model (30.42). Although having the same time constant in both systems is theoretically correct, any control practitioner would want to have the transient dynamics (30.46) evolve faster than the desired reference model. In other words, the transients must die out quickly, relative to the dynamics of the reference model trajectories. This design requirement is identical to the one that takes place during the construction of asymptotic state observers, originally developed by Luenberger in his PhD thesis at Stanford (1963). Per Luenberger, the reference model in (30.42) represents an open-loop observer. So, just like in choosing the closed-loop observer dynamics, one can add an error feedback term to the reference model and arrive at the observer-like reference model:

$$\dot{x}_{\text{ref}} = a_{\text{ref}} x_{\text{ref}} + b_{\text{ref}} r + \boxed{k_e(x - x_{\text{ref}})} \quad (30.74)$$

Error Feedback Term

where $k_e > 0$ is the reference model feedback gain. The newly introduced error feedback term in (30.74) is equivalent to the output innovation feedback in a state observer. It is easy to see that in this case, the corresponding error dynamics become faster than the open-loop reference model from (30.42):

$$\dot{e} = (a_{\text{ref}} - k_e) e + b (\Delta k_x x + \Delta k_r r) \quad (30.75)$$

Once again, Lyapunov-based arguments can be easily repeated to prove (a) global asymptotic stability of the modified error dynamics (30.74) and (b) uniform boundedness of all signals in the related closed-loop system. Readers familiar with the MRAC stability proof concept should recognize that using the same Lyapunov function candidate (30.47), one needs to compute its time derivative along the trajectories of (30.75), substitute the adaptive law from (30.42), and then show that the resulting time derivative is globally nonpositive. This will prove uniform boundedness of the tracking error e and of the parameter estimation errors (30.45). Furthermore, since in the observer-like reference model (30.74), $a_{\text{ref}} < 0$ and the error feedback term is bounded, then the model state x_{ref} is bounded as well. The rest of the proof follows standard (in MRAC) stability arguments, finally arriving at (30.48).

Revised block-diagram with the observer-like reference model (30.74) is shown in Fig. 30.7.

As the reference model error feedback gain k_e is increased, the system transient dynamics become less oscillatory. In order to gain further insights into the transient behavior, choose $k_0 > 0$, a small positive parameter ε , and redefine the reference model feedback gain:

$$k_e = \frac{k_0}{\varepsilon} \quad (30.76)$$

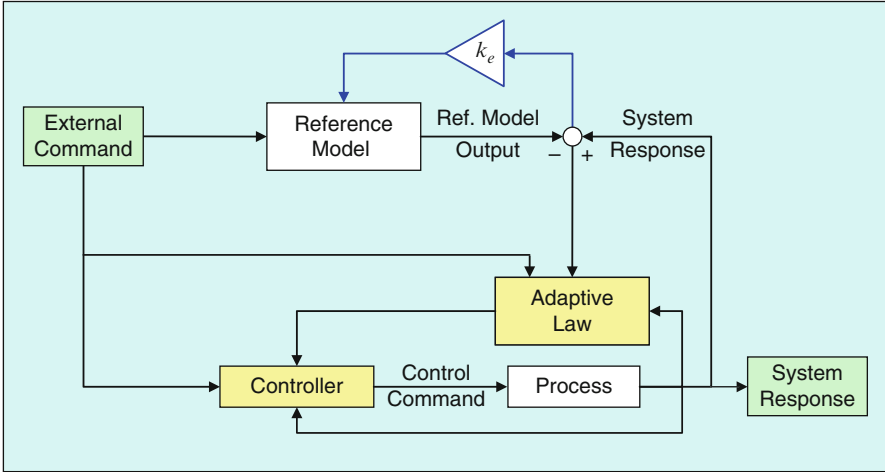


Fig. 30.7 MRAC block-diagram with observer-like reference model

Then the modified error dynamics (30.75) become

$$\varepsilon \dot{e} = (\varepsilon a_{\text{ref}} - k_0) e + \varepsilon \underbrace{[b (\Delta k_x x + \Delta k_r r)]}_{\varphi(t)} \tag{30.77}$$

Since all signals in the closed-loop system are uniformly bounded, it is not difficult to show that there exists a strictly positive finite constant $0 < \varphi_{\text{max}} < \infty$ such that for any $\varepsilon > 0$, the upper bound $|\varphi(t)| \leq \varphi_{\text{max}}$ holds uniformly in time and ε . Furthermore, starting from an initial condition $e(0) = e_0$, the solution of (30.77) can be written explicitly:

$$e(t) = e^{(a_{\text{ref}} - \frac{k_0}{\varepsilon})t} e(0) + \int_0^t e^{(a_{\text{ref}} - \frac{k_0}{\varepsilon})(t-\tau)} \varphi(\tau) d\tau \tag{30.78}$$

and one can compute an upper bound for this signal:

$$|e(t)| \leq e^{-k_0 \frac{t}{\varepsilon}} |e_0| + \frac{\varphi_{\text{max}}}{k_0} \varepsilon \tag{30.79}$$

This relation is valid for any fixed $\varepsilon > 0$ uniformly in time. So, the system state $x(t)$ converges within $(\pm \frac{\varphi_{\text{max}}}{k_0} \varepsilon)$ of the reference model state $x_{\text{ref}}(t)$ exponentially fast and at the rate no slower than $e^{-k_0 \frac{t}{\varepsilon}}$. This term gives an upper-bound quantification for the decay rate of the MRAC transient dynamics due to initial conditions mismatch $x(0) \neq x_{\text{ref}}(0)$. Otherwise, the system transients would remain within

ε -dependent bounds $\left(\pm \frac{\varphi_{\max}}{k_0} \varepsilon\right)$. Consequently, the system transients are reduced by decreasing ε , which according to (30.76) corresponds to increasing the reference model feedback gain k_e . Being able to influence and shape the MRAC transient dynamics constitutes the essential benefit of the Luenberger-like reference model modification (30.74)–(30.76). Relation (30.79) can also be written as

$$x(t) = x_{\text{ref}}(t) + C e^{-k_e t} + o(1) \tag{30.80}$$

where $C > 0$ is a constant independent of k_e and $o(1)$ is the “small-O” signal (a function of time that decays to zero asymptotically, as $t \rightarrow \infty$). The second term in (30.80) defines the transient dynamics due to initial conditions. Consequently, with a large enough feedback gain k_e , MRAC transient dynamics can be quantified and forced to decay as fast as needed. Note that since k_e is inversely proportional to ε , then the obvious trade-off in the modified MRAC design would be to avoid high gain effects in the reference model.

As for standard MRAC, it is also possible to generalize the observer-based MRAC to a broad class of nonlinear MIMO uncertain dynamical systems in the form

$$\begin{aligned} \underbrace{\begin{pmatrix} \dot{e}_{yI} \\ \dot{x}_p \end{pmatrix}}_{\dot{x}} &= \underbrace{\begin{pmatrix} 0_{m \times m} & C_p \\ 0_{n_p \times m} & A_p \end{pmatrix}}_A \underbrace{\begin{pmatrix} e_{yI} \\ x_p \end{pmatrix}}_x + \underbrace{\begin{pmatrix} 0_{m \times m} \\ B_p \end{pmatrix}}_B \Lambda \left(u + \overbrace{\Theta_d^T \Phi_d(x_p)}^{d(x_p)} \right) + \underbrace{\begin{pmatrix} -I_{m \times m} \\ 0_{n_p \times m} \end{pmatrix}}_{B_{\text{ref}}} y_{\text{cmd}} \\ y &= \underbrace{\begin{pmatrix} 0_{m \times m} & C_p \end{pmatrix}}_C x \end{aligned} \tag{30.81}$$

These dynamics incorporate an n_p -dimensional open-loop system with m control inputs u - and m - regulated outputs y . This is the original plant, whose state is $x_p \in R^{n_p}$. The plant is augmented by the m -dimensional integrated output tracking error dynamics $\dot{e}_{yI} = C_p x_p - y_{\text{cmd}}$, where $C_p \in R^{m \times n_p}$ is a known constant matrix. The order of the complete system (30.81) is $n = n_p + m$. In addition, $x \in R^n$ is the system state vector, $u \in R^m$ is the control input, $y \in R^p$ is the regulated output, $y_{\text{cmd}} \in R^m$ is the commanded signal for y to follow, $d(x_p) = \Theta_d^T \Phi_d(x_p) \in R^m$ is a nonlinear state-dependent matched parametric uncertainty, $\Theta_d \in R^{N \times m}$ is the matrix of unknown constant “true” parameters, and $\Phi_d(x_p) \in R^N$ is the known N -dimensional regressor vector, whose components are locally Lipschitz continuous in x , that is, there exists a finite positive known constant $0 < L_{\Phi_d} < \infty$ such that for any $(x_1, x_2) \in R^{n_p}$ from a bounded neighborhood of the origin, the following inequality holds

$$\|\Phi_d(x_1) - \Phi_d(x_2)\| \leq L_{\Phi_d} \|x_1 - x_2\| \tag{30.82}$$

Also in (30.81), $A \in R^{n \times n}$, $B \in R^{n \times m}$, $B_{\text{ref}} \in R^{n \times m}$, and $C \in R^{m \times n}$ are constant known matrices, while $\Lambda \in R^{m \times m}$ is a constant diagonal unknown matrix with strictly positive diagonal elements.

Consideration of the process dynamics (30.81) is largely motivated by aerospace applications, where x_p models the 6-DoF motion of an airborne platform and $d(x_p)$ represents uncertainties in the vehicle aerodynamic moments. By definition, the moment uncertainties appear together with the system control inputs, thus enforcing the matching conditions needed to justify mere existence of a control solution. Moreover, control actuator uncertainties, control effectiveness reduction, and other control failures are modeled by an unknown constant matrix Λ . Finally, inclusion of the integrated output tracking error $\dot{e}_{y_I} = C_p x_p - y_{\text{cmd}}$ into the open-loop system leads to the extended system formulation (30.81). This inclusion is optional, yet it allows the designer to explicitly account for baseline controllers with integral feedback, and it also allows to avoid feedforward terms in a control solution. Other dynamics, such as structural notch filters, sensors, and actuators, can also be added in the formulation of the extended open-loop system.

In order to control a dynamical system such as (30.81), one needs the nominal system (no uncertainties) to be controllable. It is well known that controllability of (A_p, B_p) , coupled with the rank condition,

$$\text{rank} \begin{pmatrix} A_p & B_p \\ C_p & 0_{p \times m} \end{pmatrix} = n_p + m = n \quad (30.83)$$

ensures controllability of the extended pair (A, B) . Disregarding the system uncertainties, it is straightforward to form the ideal reference model dynamics:

$$\dot{x}_{\text{ref ideal}} = A_{\text{ref}} x_{\text{ref ideal}} + B_{\text{ref}} y_{\text{cmd}} \quad (30.84)$$

where

$$A_{\text{ref}} = A - B \underbrace{\left(R_{\text{ref}}^{-1} B^T P_{\text{ref}} \right)}_{K_{\text{lqr}}^T} \quad (30.85)$$

is Hurwitz, K_{lqr} is the baseline LQR feedback gain, P_{ref} is the unique symmetric positive definite solution of the ARE,

$$P_{\text{ref}} A + A^T P_{\text{ref}} - P_{\text{ref}} B R_{\text{ref}}^{-1} B^T P_{\text{ref}} + Q_{\text{ref}} = 0 \quad (30.86)$$

and $(Q_{\text{ref}}, R_{\text{ref}})$ are some appropriately chosen symmetric positive definite matrices. Using the LQR design is the preferred way to formulate reference model dynamics and to embed basic performance of an LQR PI controller into system specifications. Due to inclusion of the integrated tracking error in (30.81), the DC gain of the reference model (30.84) is unity. Consequently, if $\Lambda = I_{m \times m}$ and $d(x) = 0_{m \times 1}$, then the baseline LQR PI linear state feedback control $u_{\text{lqr}} = -K_{\text{lqr}}^T x$ enforces global exponential stability of the reference model (30.84), and it makes the regulated output $y(t)$ track any bounded command $y_{\text{cmd}}(t)$, with bounded errors. For a step-input command, the LQR PI controller provides global exponential tracking with zero steady-state errors. Also, it is easy to see that such a choice of the reference model enforces the model matching conditions, whereby given a

Hurwitz matrix A_{ref} and an unknown constant positive definite diagonal matrix Λ , there exists a constant possibly unknown gain matrix K_x such that

$$A_{\text{ref}} = A - B \Lambda K_x^T \quad (30.87)$$

It is important to understand that in this case, existence of K_x is guaranteed for any controllable pair (A, B) and for any nonsingular matrix Λ . In particular, relations (30.85) and (30.87) imply

$$K_x = K_{\text{lqr}} \Lambda^{-1} \quad (30.88)$$

Using (30.87), it is convenient to rewrite the system dynamics (30.81) in the form

$$\dot{x} = A_{\text{ref}} x + B \Lambda \left(u + \underbrace{\left[K_x^T x + \Theta_d^T \Phi_d(x_p) \right]}_{\Theta^T} \right) + B_{\text{ref}} y_{\text{cmd}} \quad (30.89)$$

$$\underbrace{\left(K_x^T \ \Theta_d^T \right)}_{\Theta^T} \underbrace{\begin{pmatrix} x \\ \Phi_d(x_p) \end{pmatrix}}_{\Phi(x)}$$

and then get

$$\dot{x} = A_{\text{ref}} x + B \Lambda \left(u + \Theta^T \Phi(x) \right) + B_{\text{ref}} y_{\text{cmd}} \quad (30.90)$$

The control goal of interest is bounded tracking of y_{cmd} in the presence of the system parametric uncertainties $\{\Lambda, \Theta\}$. Specifically, one needs to find a control input u such that the regulated output $y = C x \in R^m$ tracks any bounded time-varying command $y_{\text{cmd}}(t) \in R^m$ with bounded errors, while the rest of the signals in the corresponding closed-loop system remain bounded. In addition, it is desirable to have smooth and quantifiable transient characteristics in the closed-loop dynamics. Using Lyapunov-based arguments (Khalil 1996), coupled with asymptotic analysis (Kevorkian and Cole 1996), one can derive MRAC systems with quantifiable transient performance.

Similar to (30.74) and for the system dynamics (30.90), consider a Luenberger-like reference model in the form

$$\dot{x}_{\text{ref}} = A_{\text{ref}} x_{\text{ref}} + \underbrace{\left[L_v(x - x_{\text{ref}}) \right]}_{\text{Error Feedback Term}} + B_{\text{ref}} y_{\text{cmd}} \quad (30.91)$$

where $\hat{x} \in R^n$ is the reference model state and $L_v \in R^{n \times n}$ is the error feedback gain, parameterized by a positive scalar $v > 0$ (to be defined). The system control input u is selected as

$$u = -\hat{\Theta}^T \Phi(x) \quad (30.92)$$

Substituting (30.92) into the system dynamics (30.90) gives

$$\dot{x} = A_{\text{ref}} x - B \Lambda \underbrace{\left(\hat{\Theta} - \Theta^T \right)}_{\Delta\Theta} \Phi(x) + B_{\text{ref}} y_{\text{cmd}} \quad (30.93)$$

where $\Delta\Theta \in R^{N \times m}$ denotes the matrix of parameter estimation errors.

In what follows, the pair $(L_v, \hat{\Theta})$ will be selected such that the system state x globally asymptotically tracks x_{ref} – the state of the observer-like reference model (30.91), and so $y \xrightarrow{t \rightarrow \infty} y_{\text{ref}}$. Also, one can show that x_{ref} tracks $x_{\text{ref ideal}}$, which in turn implies that $y_{\text{ref}} \xrightarrow{t \rightarrow \infty} y_{\text{ref ideal}}$. Furthermore, since the output of the ideal reference model (30.84) follows its command $y_{\text{ref ideal}} \rightarrow y_{\text{cmd}}$, with bounded errors, and $y \xrightarrow{t \rightarrow \infty} y_{\text{ref}} \xrightarrow{t \rightarrow \infty} y_{\text{ref ideal}}$, then the system-regulated output y will also track y_{cmd} with bounded errors. This argument constitutes the proposed design strategy.

Begin by choosing adaptive laws for $\hat{\Theta}$ so that x globally asymptotically tracks x_{ref} , in the presence of the system uncertainties. Let,

$$e = x - x_{\text{ref}} \quad (30.94)$$

denote the state tracking error. Subtracting (30.91) from (30.93), gives the system transient dynamics:

$$\dot{e} = (A_{\text{ref}} - L_v) e - B \Lambda \Delta \Theta^T \Phi(x) \quad (30.95)$$

Choose the error feedback gain L_v as

$$L_v = P_v R_v^{-1} \quad (30.96)$$

where $P_v = P_v^T > 0$ is the unique solution of the following ARE,

$$P_v A_{\text{ref}}^T + A_{\text{ref}} P_v - P_v R_v^{-1} P_v + Q_v = 0 \quad (30.97)$$

with the ARE weight matrices (Q_v, R_v) selected as

$$Q_v = Q_0 + \left(\frac{\nu + 1}{\nu} \right) I_{n \times n}, \quad R_v = \frac{\nu}{\nu + 1} I_{n \times n} \quad (30.98)$$

using a constant parameter $\nu > 0$. This constant will eventually become the design “tuning knob,” where small values of ν yield better MRAC transients. However, the corresponding feedback gain L_v will increase at the rate of $\frac{1}{\nu}$. In fact, as ν tends to zero, the error feedback gain tends to infinity:

$$L_v = \left(1 + \frac{1}{\nu} \right) P_v = O\left(\frac{1}{\nu} \right) \quad (30.99)$$

while the solution P_v of the ARE (30.97) tends to a constant positive definite symmetric matrix P_0 . It is easy to verify that the ARE (30.97) possesses the unique symmetric positive definite solution P_v . Furthermore, because of (30.97), the observer closed-loop matrix

$$A_v = A_{\text{ref}} - L_v = A_{\text{ref}} - P_v R_v^{-1} = A_{\text{ref}} - P_v \left(1 + \frac{1}{v}\right) \quad (30.100)$$

satisfies

$$P_v \underbrace{\left(A_{\text{ref}} - \underbrace{P_v R_v^{-1}}_{L_v} \right)}_{A_v}^T + \underbrace{\left(A_{\text{ref}} - \underbrace{P_v R_v^{-1}}_{L_v} \right)}_{A_v} P_v + P_v R_v^{-1} P_v + Q_v = 0 \quad (30.101)$$

or equivalently

$$P_v A_v^T + A_v P_v = -P_v R_v^{-1} P_v - Q_v < 0 \quad (30.102)$$

and therefore, A_v is Hurwitz for any $v > 0$.

Since P_v is the unique symmetric positive definite solution of the ARE (30.97), then the matrix inverse $\tilde{P}_v = P_v^{-1}$ exists for any $v \geq 0$ and the following relation takes place:

$$A_v^T \tilde{P}_v + \tilde{P}_v A_v = -R_v^{-1} - \tilde{P}_v Q_v \tilde{P}_v < 0 \quad (30.103)$$

The design task is to choose adaptive laws for $\hat{\Theta}$ so that the tracking error e globally asymptotically tends to the origin. Toward that end, consider the following Lyapunov function candidate:

$$V(e, \Delta\Theta) = e^T \tilde{P}_v e + \text{trace}(\Lambda \Delta\Theta^T \Gamma_{\Theta}^{-1} \Delta\Theta) \quad (30.104)$$

where $\Gamma_{\Theta} = \Gamma_{\Theta}^T > 0$ is the adaptation rate. The time derivative of V , along the trajectories of the error dynamics (30.95), can be computed as

$$\begin{aligned} \dot{V}(e, \Delta\Theta) &= e^T \tilde{P}_v \dot{e} + \dot{e}^T \tilde{P}_v e + 2 \text{trace}(\Lambda \Delta\Theta^T \Gamma_{\Theta}^{-1} \dot{\Theta}) \\ &= e^T \tilde{P}_v (A_v e - B \Lambda \Delta\Theta^T \Phi(x)) + (A_v e - B \Lambda \Delta\Theta^T \Phi(x))^T \tilde{P}_v e \\ &\quad + 2 \text{trace}(\Lambda \Delta\Theta^T \Gamma_{\Theta}^{-1} \dot{\Theta}) \\ &= e^T (\tilde{P}_v A_v + A_v^T \tilde{P}_v) e - 2e^T \tilde{P}_v B \Lambda \Delta\Theta^T \Phi(x) \\ &\quad + 2 \text{trace}(\Lambda \Delta\Theta^T \Gamma_{\Theta}^{-1} \dot{\Theta}) \end{aligned} \quad (30.105)$$

Because of (30.102) and using the properties of the matrix trace operator,

$$\dot{V}(e, \Delta\Theta) = -e^T (R_v^{-1} + \tilde{P}_v Q_v \tilde{P}_v) e + 2 \text{trace}(\Lambda \Delta\Theta^T (\Gamma_{\Theta}^{-1} \dot{\Theta} - \Phi(x) e^T \tilde{P}_v B)) \quad (30.106)$$

If the adaptive laws are chosen as

$$\dot{\Theta} = \Gamma_{\Theta} \Phi(x) e^T \tilde{P}_v B \quad (30.107)$$

then

$$\dot{V}(e, \Delta\Theta) = -e^T (R_v^{-1} + \tilde{P}_v Q_v \tilde{P}_v) e \leq 0 \quad (30.108)$$

and, hence, $V(e, \Delta\Theta)$ is the Lyapunov function for the error dynamics (30.95). For this reason, the tracking error signal e as well as the parameter error matrix $\Delta\Theta$ are uniformly bounded in time, that is, $(e, \Delta\Theta) \in L_\infty$. Since A_{ref} in (30.91) is Hurwitz by design and $(e, y_{\text{cmd}}) \in L_\infty$, then $(x_{\text{ref}}, \dot{x}_{\text{ref}}) \in L_\infty$ and consequently $x \in L_\infty$. Since the unknown parameters Θ are constant and $\Delta\Theta \in L_\infty$ then $\hat{\Theta} \in L_\infty$. The regressor vector $\Phi(x_p)$ is Lipschitz continuous and $(x, \hat{\Theta}) \in L_\infty$. Therefore, from definition (30.92) it follows that $u \in L_\infty$ and consequently $\dot{x} \in L_\infty$. Also, since $\dot{x}_{\text{ref}} \in L_\infty$, then $\dot{e} \in L_\infty$. Using (30.108) yields

$$\ddot{V}(e, \Delta\Theta) = -2e^T (R_v^{-1} + \tilde{P}_v Q_v \tilde{P}_v) \dot{e} \in L_\infty \quad (30.109)$$

The function V from (30.104) is lower bounded and has a nonincreasing time derivative as in (30.108). Thus, V tends to a limit, as $t \rightarrow \infty$. Also the function's second time derivative is uniformly bounded. Therefore, \dot{V} is a uniformly continuous function of time. Using Barbalat's lemma (Khalil 1996) implies that $\dot{V}(t)$ tends to zero, as $t \rightarrow \infty$. Finally, and due to (30.108),

$$\lim_{t \rightarrow \infty} \|e(t)\| = 0 \quad (30.110)$$

which proves global asymptotic stability of the tracking error, attained by the adaptive controller (30.92), the adaptive laws (30.107), and the observer-like reference model (30.91).

In order to show that x_{ref} asymptotically tracks $x_{\text{ref ideal}}$, it is sufficient to subtract (30.84) from (30.91) and write the dynamics of the reference model error $e_{\text{ref}} = x_{\text{ref}} - x_{\text{ref ideal}}$:

$$\dot{e}_{\text{ref}} = A_{\text{ref}} e_{\text{ref}} + L_v \underbrace{e(t)}_{\text{o}(1)} \quad (30.111)$$

Then,

$$e_{\text{ref}}(t) = \exp(A_{\text{ref}} t) e_{\text{ref}}(0) + \int_0^t \exp(A_{\text{ref}}(t-\tau)) L_v \underbrace{e(\tau)}_{\text{o}(1)} d\tau = \text{o}(1) \xrightarrow{t \rightarrow \infty} 0 \quad (30.112)$$

So $x \xrightarrow{t \rightarrow \infty} x_{\text{ref}} \xrightarrow{t \rightarrow \infty} x_{\text{ref ideal}}$, and hence,

$$(y = C x) \xrightarrow{t \rightarrow \infty} (y_{\text{ref}} = C x_{\text{ref}}) \xrightarrow{t \rightarrow \infty} (y_{\text{ref ideal}} = C x_{\text{ref ideal}}) \rightarrow y_{\text{cmd}}(t) \quad (30.113)$$

In other words, the system-regulated output y asymptotically tracks its ideal reference command $y_{\text{ref ideal}}$, and y also tracks its original command y_{cmd} with bounded errors.

Table 30.4 Observer-based MRAC design summary

Open-loop plant	$\dot{x} = A_{\text{ref}} x + B \Lambda (u + \Theta^T \Phi(x)) + B_{\text{ref}} y_{\text{cmd}}$
Observer-like reference model	$\dot{x}_{\text{ref}} = A_{\text{ref}} x_{\text{ref}} + L_v (x - x_{\text{ref}}) + B_{\text{ref}} y_{\text{cmd}}$
State tracking error	$e = x - x_{\text{ref}}$
Riccati equation for adaptive laws	$P_v A_{\text{ref}}^T + A_{\text{ref}} P_v - P_v R_v^{-1} P_v + Q_v = 0$
ARE weight matrices	$Q_v = Q_0 + \left(\frac{v+1}{v}\right) I_{n \times n}, \quad R_v = \frac{v}{v+1} I_{n \times n}$
Observer gain	$L_v = P_v R_v^{-1}$
Total control input	$u = -\hat{\Theta}^T \Phi(x)$
MRAC laws	$\dot{\hat{\Theta}} = \Gamma_{\Theta} \Phi(x) e^T P_v^{-1} B$

The design summary is given in Table 30.4.

In order to analyze the transient dynamics (30.95), substitute (30.96) into (30.95) and write the transient error dynamics as

$$\dot{e} = \underbrace{(A_{\text{ref}} - P_v R_v^{-1})}_{\text{Hurwitz Matrix}} e - \underbrace{B \Lambda \Delta \Theta(t)^T \Phi(x(t))}_{\varphi(t) = \text{Uniformly Bounded Function of Time}} \quad (30.114)$$

Using (30.98) gives

$$\dot{e} = \left(A_{\text{ref}} - \left(1 + \frac{1}{v} \right) P_v \right) e - \varphi(t) \quad (30.115)$$

In (Lavretsky 2011), it is shown that the asymptotic relation

$$P_v = P_0 + O(v), \quad \text{as } v \rightarrow 0 \quad (30.116)$$

holds with a constant positive definite symmetric matrix P_0 . Then,

$$\dot{e} = \left(A_{\text{ref}} - \left(1 + \frac{1}{v} \right) (P_0 + O(v)) \right) e - \varphi(t) \quad (30.117)$$

or equivalently

$$v \dot{e} = (v A_{\text{ref}} - (v+1)(P_0 + O(v))) e - v \varphi(t) \quad (30.118)$$

Rewrite (30.118) as

$$\begin{aligned} v \dot{e} &= (v A_{\text{ref}} - (v+1)(P_0 + O(v))) e - v \varphi(t) \\ &= \left(-P_0 + \underbrace{(v A_{\text{ref}} - v(P_0 + O(v)) - O(v))}_{O(v)} \right) e + v \varphi(t) \\ &= (-P_0 + O(v)) e + v \varphi(t) \end{aligned} \quad (30.119)$$

or, equivalently,

$$\dot{e} = \frac{1}{\nu} (-P_0 + O(\nu)) e + \varphi(t) \quad (30.120)$$

It is not difficult to show (by direct integration), that solutions of (30.120) satisfy the following asymptotics

$$e(t) = O\left(e^{-\gamma \frac{t}{\nu}}\right) + O(\nu), \quad (\nu \rightarrow 0) \quad (30.121)$$

uniformly in time, with a positive constant γ and for all sufficiently small $\nu > 0$. So, the transient dynamics exponentially decay to a neighborhood of the origin, no slower than $O\left(e^{-\gamma \frac{t}{\nu}}\right)$. Moreover, the “diameter” of the convergence set can be made arbitrarily small, by choosing ν to be sufficiently small. This argument formally proves and quantifies transient dynamics improvements in MIMO MRAC systems with observer-like reference models.

There is also an alternative way to analyze the transient dynamics in (30.118). This system can be viewed as singularly perturbed, where ν plays the role of a small parameter. To understand the intricacies of the system behavior, one can employ the singular perturbation arguments (Khalil 1996; Kevorkian and Cole 1996). Setting $\nu = 0$ gives the isolated root $e = 0$ for the corresponding reduced system, which describes asymptotic behavior as $t \rightarrow \infty$, that is, for a sufficiently small $\nu > 0$, the error trajectories converge to a small neighborhood of the manifold $e \equiv 0$ and will evolve near this manifold thereafter. Next, the boundary-layer system is formed to quantify and characterize the transient dynamics. These dynamics are derived by “stretching” the time

$$\tau = \frac{t}{\nu} \quad (30.122)$$

rewriting (30.118) in the “fast” time scale τ , and then setting $\nu = 0$. The resulting boundary-layer dynamics

$$\frac{d e}{d \tau} = -P_0 e \quad (30.123)$$

are globally exponentially stable, since P_0 is symmetric and positive definite (Kevorkian and Cole 1996). In this case, one can claim (Khalil 1996) that for a sufficiently small $\nu > 0$, while starting from an initial time $t_0 \geq 0$, the singular perturbation system (30.118) has a unique solution $e(t, \nu)$, defined on an infinite interval $[t_0, \infty)$, and the asymptotic relation

$$e(t, \nu) = \bar{e}\left(\frac{t}{\nu}\right) + O(\nu) \quad (30.124)$$

holds uniformly on $[t_0, \infty)$, where $\bar{e}\left(\frac{t}{\nu}\right)$ is the solution of the boundary-layer system (30.123) and $t_0 > 0$ is the initial time instant. Since,

$$\bar{e}\left(\frac{t}{\nu}\right) = \exp(-P_0(t - t_0)) \bar{e}(0) \quad (30.125)$$

then substituting (30.125) into (30.124) results in

$$e(t, \nu) = \exp\left(-P_0 \left(\frac{t-t_0}{\nu}\right)\right) (x(t_0) - x_{\text{ref}}(t_0)) + O(\nu) \tag{30.126}$$

This asymptotic relation is conservative. In fact, it has been already proven that the tracking error $e(t, \nu)$ asymptotically converges to the origin, starting from any initial condition. Consequently,

$$\varphi(t) = B \Lambda \underbrace{\left[\Delta\Theta(t)^T \Phi(x(t))\right]}_{o(1)} = o(1), \quad (t \rightarrow \infty) \tag{30.127}$$

and so, (30.126) can be rewritten as

$$x(t, \nu) = \underbrace{\exp\left(-P_0 \left(\frac{t-t_0}{\nu}\right)\right) (x(t_0) - x_{\text{ref}}(t_0))}_{\text{Transient Dynamics}} + \underbrace{x_{\text{ref}}(t) + O(\nu)o(1)}_{\text{Global Asymptotic Stability}} \tag{30.128}$$

where P_0 is a constant symmetric positive definite matrix, $o(1)$ is a function of time with $\lim_{t \rightarrow \infty} o(1) = 0$, and $O(\nu)$ decays to zero no slower than ν . Design details and stability proofs can be found in (Lavretsky 2011).

The asymptotic expansion (30.128) quantifies the MRAC transient dynamics. Indeed, for a sufficiently small $\nu > 0$, the transients, described by the first term in (30.128), decay exponentially fast, while the second term defines asymptotic behavior of the tracking error, as $t \rightarrow \infty$. This constitutes the main benefit of using the error feedback in an observer-based reference model. Essentially, with a sufficiently small parameter $\nu > 0$, one ensures quantifiable transient characteristics, and the latter are given by the first term in (30.128). The observer-based MRAC design method represents a numerically efficient technique of reducing unwanted transient oscillations in state feedback/feedforward MRAC systems.

The plant dynamics (30.81) and the corresponding control problem formulations can be modified to include nonparametric uncertainties, such as matched uncertainty approximation errors and bounded possibly nonmatched process noise. In that case, one can use known robustification techniques (i.e., σ -modification, e -modification, and the projection operator) to prove bounded tracking performance and then establish transient characteristics. Also, the state feedback MRAC design, with an observer-like reference model, can be extended to adaptive output feedback controllers (Lavretsky 2012).

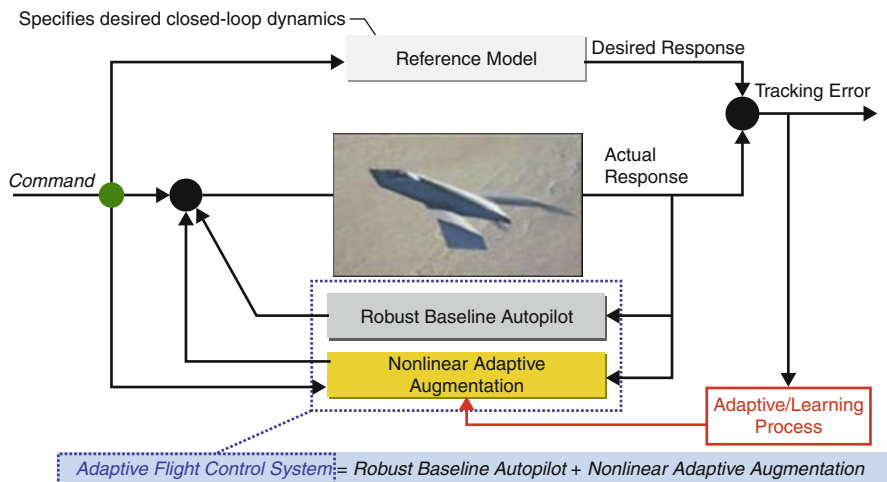


Fig. 30.8 (Robust + adaptive) flight control system

30.6 Conclusion

Robust and adaptive methods can be seamlessly combined to construct resilient controllers, applicable to a wide range of systems, including aerial platforms. A notional block-diagram is shown in Fig. 30.8.

This system is designed to track and execute external commands, provided by a pilot, a guidance logic, or an autonomous mission planner. The architecture embeds a robust baseline controller (LQR PI feedback). The reference model represents the baseline closed-loop dynamics that would be achieved under the baseline controller and without uncertainties. The adaptive control acts as an augmentation to the baseline. Its purpose is to recover the desired baseline performance while operating in the presence of “unknown unknowns” in the system dynamics and operational environment. As depicted in the figure, this control architecture was designed and flown on various vehicles at the Boeing Company. Some are in production today, and yet others were designed to test and verify extreme capabilities and resilience of aerial platforms equipped with robust and adaptive flight controllers.

References

- R.L. Butchart, B. Shackcloth, Synthesis of model reference adaptive control systems by Lyapunov’s second method, in *Proceedings of 1965 IFAC Symposium on Adaptive Control*, Teddington, UK, 1965
- B. Etkin, *Dynamics of flight. Stability and control*, 2nd edn. (Wiley, New York, 1982)

- G.F. Franklin, J.D. Powell, A. Emami-Naeni, *Feedback Control of Dynamic Systems* (Addison-Wesley, Reading, 1986)
- P. Ioannou, P. Fidan, *Adaptive Control Tutorial*. Advances in Design and Control (SIAM, Philadelphia, 2006)
- J. Kevorkian, J.D. Cole, *Multiple Scale and Singular Perturbation Methods*. Applied Mathematical Sciences, vol 114 (Springer, New York, 1996)
- H. Khalil, *Nonlinear Systems*, 3rd edn. (Prentice Hall, Upper Saddle River, 1996)
- E. Lavretsky, Reference dynamics modification in adaptive controllers for improved transient performance, in *Proceedings of AIAA Guidance, Navigation and Control Conference*, Portland, OR, 2011
- E. Lavretsky, Adaptive output feedback design using asymptotic properties of LQG/LTR Controllers. *IEEE Trans. Autom. Control* **57**(6), 1587–1591 (2012)
- D. McRuer, I. Ashkenas, D. Graham, *Aircraft Dynamics and Automatic Control* (Princeton University Press, Princeton, 1990)
- K.S. Narendra, A.M. Annaswamy, *Stable Adaptive Control* (Dover, New York, 2005)
- P.D. Parks, Lyapunov redesign of model reference adaptive systems. *IEEE Trans. Autom. Control* **11**, 362–367 (1966)
- J.-J.E. Slotine, W. Li, *Applied Nonlinear Control* (Prentice Hall, Englewood Cliffs, 1995)
- B.L. Stevens, F.L. Lewis, *Aircraft Control and Simulation* (Wiley, New York, 1992)
- H.P. Whitaker, J. Yamron, A. Kezer, Design of Model-Reference Control Systems for Aircraft, Rep. R-164, Instrumentation Laboratory, MIT, Cambridge, MA (1958)